ISSN(Online):2045-8711
ISSN(Print):2045-869x

July 2011 No.1 vol.7

International Journal of Innovative Technology & Creative Engineering

UK: Managing Editor
International Journal of Innovative Technology and Creative Engineering
1a park lane,
Cranford
London
TW59WA
UK
E-Mail: editor@ijitce.co.uk
Phone: +44-773-043-0249

USA: Editor
International Journal of Innovative Technology and Creative Engineering
Dr. Arumugam
Department of Chemistry
University of Georgia
GA-30602, USA.
Phone: 001-706-206-0812
Fax:001-706-542-2626

India: Editor
International Journal of Innovative Technology & Creative Engineering
Dr. Arthanariee. A. M
Finance Tracking Center India
261 Mel quarters
Labor colony,
Guindy,
Chennai -600032.
Mobile: 91-7598208700

IJITCE PUBLICATION

INTERNATIONAL JOURNAL OF INNOVATIVE TECHNOLOGY & CREATIVE ENGINEERING

Vol.1 No.7

July 2011

www.ijitce.co.uk

From Editor's Desk

Dear Researcher,

Greetings!

Research articles in this issue discusses about Multi-agent Q Learning, Artificial Neural Networks, Flow of Herschel, Euclidean distance on sonographic image.
Let us see some happenings of month July around us, The Energy Sciences Network (ESnet) announced a major step toward creating one of the world's fastest and most advanced scientific networks to accelerate U.S. competitiveness in science and technology. Known as the Advanced Networking Initiative (ANI), the effort represents a $62 million multi-year investment

The 13-day mission saw the Atlantis crew deliver food and other vital supplies to the International Space Station, which will now be totally reliant on Russian Soyuz spacecraft to ferry astronauts back and forth. After 135 missions into space, the shuttle fleet is today finally being retired. This is set to trigger around 3000 job losses.

It's paint-by-numbers for neuroscientists. At the Max-Planck Institute for Medical Research in Heidelberg, Germany, researchers have devised a faster way of computing the neural connections that make up the brain.
Veteran of micro computing Steve Furber, in his role as ICL Professor of Computer Engineering in the School of Computer Science at the University of Manchester, has called upon some old friends for his latest project: a brain-simulating supercomputer based on more than a million ARM processors.
Let us come to open problems in computer virus research, there are significant problems yet to be addressed, and that these require dedicated work by clever people. It has been an absolute pleasure to present you articles that you wish to read. We look forward to many more new technology-related research articles from you and your friends. We are anxiously awaiting the rich and thorough research papers that have been prepared by our authors for the next issue.

Thanks,
Editorial Team
IJITCE

Editorial Members

Review Board Members

Contents

INTERNATIONAL JOURNAL OF INNOVATIVE TECHNOLOGY & CREATIVE ENGINEERING (ISSN:2045-8711)
VOL.1 NO.7 JULY 2011

A Behavior-based Approach for Multi-agent Q-learning for Autonomous Exploration

Dip Narayan Ray [#1], Somajyoti Majumder [#2], Sumit Mukhopadhyay [*3]

[#] *Surface Robotics Lab, Central Mechanical Engineering Research Institute (CSIR)*
Durgapur, W.B. 713209, India

[1] dnray@cmeri.res.in

[2] sjm@cmeri.res.in

[*] *Department of Mechanical Engineering, National Institute of Technology*
Durgapur, W.B. 713209, India

[3] msumitnit@yahoo.co.in

***Abstract* — The use of mobile robots is being popular over the world mainly for autonomous explorations in hazardous/ toxic or unknown environments. This exploration will be more effective and efficient if the explorations in unknown environment can be aided with the learning from past experiences. Currently reinforcement learning is getting more acceptances for implementing learning in robots from the system-environment interactions. This learning can be implemented using the concept of both single-agent and multiagent. This paper describes such a multiagent approach for implementing a type of reinforcement learning using a priority based behaviour-based architecture. This proposed methodology has been successfully tested in both indoor and outdoor environments.**

Keywords: Multiagent, Reinforcement learning, Q-learning, Behavior-based robotics, Autonomous exploration

I. INTRODUCTION

Recently the field of robotics, especially the mobile robotics has been identified as on of the most important areas of research due to its huge potential for autonomous explorations in different hazardous or toxic and unapproachable domains. These exploration domains extend from underwater exploration to factory automation, polar to planetary exploration, landmine detection to unknown environment mapping. But for such explorations, the use of a mobile robot with classical control is possible if and only if the programmer or user has the prior knowledge about the environment. It is completely impossible to develop a mobile robot for explorations without knowing the environment beforehand. For such cases, the concept of learning from past experiences may provide a better strategy for explorations. The system will learn constantly from the interactions with the environment and modify the strategy of exploration accordingly. The most suitable learning in this direction is the Reinforcement learning, especially the Q-learning which uses delayed rewards [1]. The current research work proposes a new approach of autonomous exploration using multiagent Q-learning using behaviour-based robotics. This paper is organised as follows: after this introduction, related works and a few insights have been described. Then there are proposed methodology and experimental results and discussions followed by a conclusion.

II. PREVIOUS WORKS

The field of reinforcement learning [1] has been started only few years ago. Reinforcement learning is being used for various multiagent systems to solve problems with numbers of robots/ systems. Lots of works have been done mainly theoretically and using simulation. The following paragraphs describe the work done in the field of MARL.

Reference [2] uses the traditional Q-learning algorithm for multiagent system. The main interest is focused on the complex behavior of Q-learning with $\mathcal{E}$-greedy exploration in Prison-Dilemma-like games and the algorithm is able to achieve higher-than-Nash outcomes in an undiscovered chaotic system. Panait and Luke have wrote a state-of-the-art paper [3] discussing the co-operative multiagent learning in broad survey. But it clearly mentions that Reinforcement Learning methods have only theoretical proof of convergence and such convergence assumption do not hold for some real-world applications including many multi-agent system problems. The application of multi – agent for Q-learning was in [4] with the use of "Q Updates with Immediate Counterfactual Rewards-learning (QUICR –

learning) algorithm which is designed to improve both the convergence properties and performance of Q-learning. This proposed modification tries to solve the existing credit assignment problem for a multiagent system. Reference [5] reviews the main benefits and challenges of multiagent Reinforcement Learning (MARL) as well as the different viewpoints on defining the MARL learning goal. There is also discussion of MARL algorithms for fully cooperative, fully competitive and mixed tasks. Issues on how autonomous agents learn to solve dynamic tasks online have been discussed. Behaviors of several MARL algorithms have been studied in simulation environments. Littman [6] described an approach to reinforcement learning in multiagent general-sum games in which learner is told to treat each other agent as either a friend or foe. This algorithm also provides strong convergence than Nash-equilibrium-based learning rule. Case-Based Heuristically Accelerated Multiagent Reinforcement Learning (CB-HAMRL) has been proposed by Bianchi & de Màntaras [7]. This algorithm is based upon an emerging technique, Heuristic Accelerated Reinforcement Learning, in which RL methods are accelerated by making use of heuristic information. Empirical evaluation has been conducted in a simulator for the Littman's robot soccer domain. Fujii et all [8] have used multilayered reinforcement learning scheme to select the appropriate collision avoidance behaviors so as to reduce the computational power and memory capacity. This helps to move numbers of robots using LOCISS (Locally Communicable Infrared Sensory System) safely in an environment full with large numbers of static obstacles. They have also used the algorithm on a real robot. This paper [9] aims to build a team of agents on long term basis where the decision making will be done using reinforcement learning. It uses robotic soccer as a multiagent Markov Decision Process and the analysis is made in own-developed 'Karlsruhe Brainstormers' simulator. Discussions on how optimality of behaviors of agents can be defined and the difficulties associated with developing algorithms to reach such optimality have been discussed. Kim and Vadakkepat [10] have used three micro-robot soccer teams in real field for analyzing the multiagent systems from robot soccer perspective. They have also reviewed the multiagent system and the learning issues in multiagent systems from robotic soccer perspective. The action selection [11] for the cooperation and coordination among agents is an important issue for multiagent systems. In dynamic and complex environments, the modular Q-learning is proposed for selecting the right action. The modular Q-learning consists of two different parts: different learning modules and the mediator module. The mediator module selects the right action based on the Q-values obtained from different learning modules. Littman [12] has described a Q-learning like algorithm for finding optimal policies for a two agent systems with diametrically opposite goals. It basically uses a reinforcement learning approach to solve two-player-zero-sum games in which the max operator in the update step of a standard Q-learning algorithm is replaced by a minimax operator that can be evaluated by solving a linear program. Reference [13] describes a framework for using reinforcement learning on mobile robots. The main feature of the work is the use of example trajectories to bootstrap the value function approximation and splitting learning into two different phases. The first phase uses human or an example for the task and reinforcement learning system observes the states, actions and rewards by the robot. When the approximation of the value-function is done properly, the reinforcement learning in the second phase is in the control of the robot as in the standard Q-learning framework. Reference [14] is a review paper which focuses on the relation of multiagent reinforcement learning (MARL) with stochastic games. This paper has also discussed varieties of topics under MARL, ranging from proof of convergence of algorithms theoretically, develop algorithms of multiagent systems and simulate them, develop robots work to achieve certain tasks or develop social skills. The author has also hoped that combination of traditional RL solutions, applied MARL research, decision theory and game theory will open a new horizon of research.

It may be concluded from the above discussions that three types of works are reported in literature, for both single-agent and multiagent reinforcement/ Q-learning.

1) First type of papers [3, 5, 13, 14] is basically review type and discuss about the work done so far in the field. They do not propose any theory or describe any experiment.

2) Second type of papers [2, 4, 6, 7, 9, 11, 12] is theoretical based and the proposed methodologies/ algorithms or any modifications of existing algorithms have been established by simulation. Further more such types of papers can be categorized into (a) purely analytical [2, 4, 6, 11, 12] and (b) simulation based robotics [7, 9].

3) Third type of papers [8, 10, 13] are experimental based i.e. the papers discuss the use of real robots in indoor/simulated environments, although work is very limited.

Literature survey also reveals that till date no work has been carried out using robot for outdoor explorations using single agent/ multiagent reinforcement learning. The current work has tried to address this issue of autonomous outdoor exploration using multiagent Q-learning based on behavior-based robotics.

III. A FEW INSIGHTS

This current work is related mainly with behavior-based robotics, reinforcement learning (especially Q-learning), multiagent system. The following paragraphs will provide a brief idea about the above topics in nutshell.

A. Behaviour-based Robotics

The existing conventional/classical robotics has some control mechanism, which guides the end effectors to act accordingly, after it analyzes the inputs, obtained from various sensors and sends responses to those end effectors. The inputs from various sensors are used intermediately to symbolically represent the environment or action. On the basis of this environmental model planning is done and then only commands are sent to the end effecters. But if the end effecters are directly coupled to those sensors and there is an intelligent agent to control the system individually, then it will be able to take decision itself. So, this is one kind of intelligence, often looked for in robots. This behavior is often called 'Reactive' in nature like the closing of eyes due to intense light in human beings.

In behavior-based robotics four architectures are popular all over the world. They are Subsumption Architecture ([15], [16], [17], [18]), Action Selection Dynamics [19], Schema-based approach ([20], [21], [22], [23]) Process Description Language [24]. Out of which only the subsumption architecture has been used in the current research for implementation. Subsumption architecture is a layered behavior proposed by Brooks. These layers are associated with many simple behaviors. All these simple behaviors combine to form complex behaviors. The layers operate asynchronously.

B. Reinforcement learning and Q-learning

Learning is needed for forming a map/ function between the state (sensor information) and action (actuator commands). Supervised learning approaches need the model of good behaviour by a teacher. Reinforcement learning is one of the widely used online learning methods in robotics. It is sometimes called learning with the critic that gives scalar reward or punishment based on behaviors [25]. The robot learns during an action and also acts/ responds during the learning, which is neglected in supervised learning methods. The Reinforcement learning method used in most of earlier works is single agent based Q-learning [26, 27]. In single agent based Q-learning algorithm the external world is modelled as Markov Decision Process with discrete states and action spaces. It is flexible in this sense because it can learn from actions which it/ programmer doesn't suggest. This ability is often called exploration – insensitivity. After each step an agent (single) observes the state vector x_i, chooses and applies an action a_i. The system passes in state x_{i+1} and the agent receives a reinforcement $r(x_i, a_i)$. The goal of the learning is to find a policy which maximizes the sum of the future reinforcements. For a given policy π, it is noted that $a_i = \pi(x_i)$, the chosen action. The evaluation function π, noted V^π, is given by:

$$V^\pi(x) = E\{r_0 + \gamma r_1 + \gamma^2 r_2 + \ldots\ldots | \; x_0 = x; \pi\}$$
$$= E\left\{\sum_{i=0}^{\infty} \gamma^i r_i \mid x_0 = x; \pi\right\} \quad (1)$$

The discounting factor $\gamma \in [0, 1]$ smaller than 1, ensures convergence of the sum. The optimal evaluation function V* (x), is defined as follows:

$$V^*(x) = \max_{a \in A_x} [r(x,a) + \gamma \sum_y P_{xy}(a) V^*(y)]$$
$$= \max_{a \in A_x} Q^*(x,a) \quad (2)$$

Where: A_x = set of possible actions in the state x; P_{xy} = probability of passing from the state x to y by the action a; Q(x,y) represents the total reinforcement if the action a is selected in state x and if an optimal policy is chosen thereafter. It is called the quality function. Optimal policy can be found using dynamic programming if transition probabilities $P_{xy}(a)$ and the reinforcement law r(x, a) are known. Instead of using evaluation function, Watkins proposed to estimate the function Q* by the function:

(x, a) → Q(x, a) which is updated with each transition by:

$$Q(x_i, a_i) \leftarrow Q(x_i, a_i) + \beta\left[r(x_i, a_i) + \gamma \max_{v \in U x_{i+1}} Q(x_{i+1}, a) - Q(x_{i+1}, a_i)\right] \quad (3)$$

Here β is a learning parameter which must tend towards 0 when t tends towards the infinite.

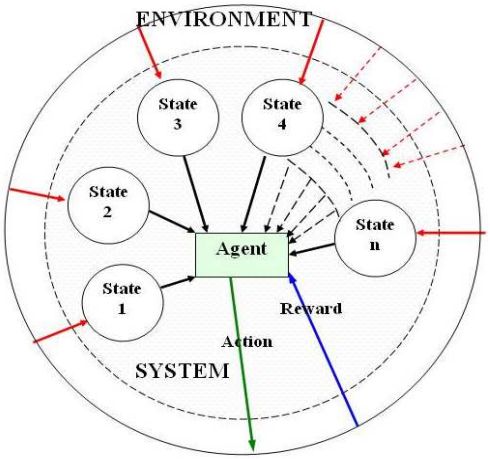

Fig. 1. System- Environment Interaction Model for Single agent Q-learning

C. Multiagent Systems

Agents are the most discussed issue for present-day advanced robotics. However this concept of agents has evolved from multi-agent system (MAS) [29] which in turn is a part of Distributed Artificial Intelligence (DAI). The (software) agent is an entity which performs continuously and autonomously particular task(s) assigned to it in an environment (populated by other agents) for achieving the desired goal. Multi-agent system is composed of multiple interactive intelligent agents that collectively complete their own individual goals to achieve the overall goal. Multi-agent system (MAS) is very useful to accomplish a complex task easily and fast. In the most general case, agents will be acting on behalf of users with different goals and motivations. To successfully interact, they will require the ability to cooperate, coordinate, and negotiate with each other, much as people do.

IV. THE PROPOSED METHODOLOGY

The proposed methodology uses the concept of gradual learning on a single agent and then a multiagent system. However the major work has been done on the multiagent system.

A. Gradual learning

The term "learning" straight forward refers mainly to human learning. Many researchers have proposed different learning models to describe human learning. It has also been mentioned that human learning relies on the past experiences. For example, the learning of day -5 depends on the learning of day-4. One cannot learn the knowledge of day-5, without the knowledge of day-4 or day-2. The knowledge of a human being is refined gradually depending up on his/ her past experience, interaction with the environment, environmental conditions. Another important inference can be drawn from the theories about human learning is that learning is in terms what he/she already knows [30]. If one doesn't understand what does 'capital' or 'country' means, he/she cannot understand that "'A' is the capital of the country 'B'". So there is one popularly used method of learning which is very much gradual/ cumulative rather than sudden. For example a child starts learning the alphabets; if first day he/ she starts learning from 'A' and stops at 'D', next day he/ she will start from 'E', not again from 'A'. This saves time and increases the efficiency of learning.

B. Human-like Gradual Multiagent Q-learning

This type of gradual learning can also be implemented for robot learning. In that case, the past experience of the robot can be referred for new or advanced learning. Q-learning, a well-known and most suitable RL for robots uses only a randomly generated Q-table for each new run. Instead of new Q-table each time, the past Q-table can be referred as initial table for second run onwards.

TABLE I
STEPS OF THE HUMAQ ALGORITHM FOR SINGLE AGENT

First run
I. Generate Q-table with random values *Repeat (forever)* *{* 1. *Read the sensor data* 2. *Decide the state (x_i) of the robot* 3. *Select the action (a) according to the state and Q-values of the corresponding action* 4. *Execute the selected action* 5. *Read the sensor data* 6. *Compute the reward/ punishment & reinforce the state – action pairs(s)* 7. *Update Q-table as final table* *}*
Second run onwards
II. Initialization: Initial Q-table = Final Q-table *Repeat (forever)* *{* 1. *Read the sensor data* 2. *Decide the state (x_i) of the robot* 3. *Select the action (a) according to the state and Q-values of the corresponding action* 4. *Execute the selected action* 5. *Read the sensor data* 6. *Compute the reward/ punishment & reinforce the state – action pairs(s)* 7. *Update Q-table as final table* *}*

In most cases, a single-agent is performing all the interactions between the system and environment

necessary for Q-learning [refer fig. 1]. But for complex situations, (say a robot with large nos. of sensors) the single-agent may not perform well. Such complex cases can be addressed by multi-agent architecture. In such cases nos. of agents individually and independently works to achieve own goal, which is a sub-part of the overall goal. When all the agents individually achieve their own goals, the main goal is achieved. Here different reactive agents have been used and the Q-tables for different agents are generated using gradual learning, except the first run.

The initial concept of Q-learning was proposed using single-agent. But later on with the advancement of robotics, multi-agent system has been developed for complex situations using several sensors. Different agents are responsible for different sensors.

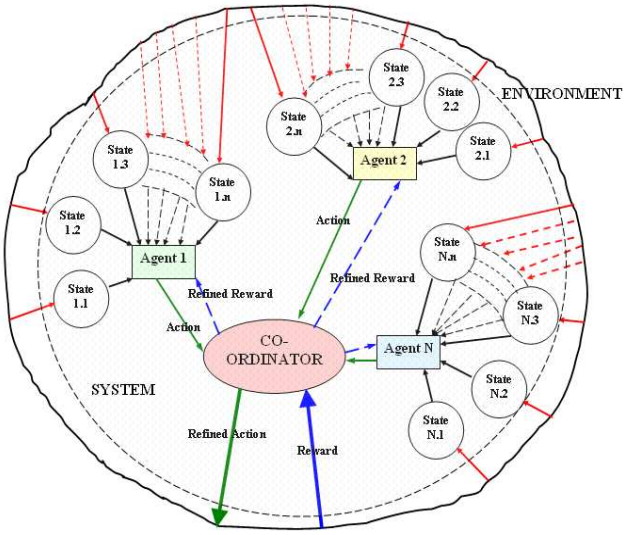

Fig. 2. Proposed Generalized Multi-agent Q-learning for a System. The system is divided in two main parts: different Agents and the Co-ordinator. System interacts with the environment with the help of Co-ordinator.

Human-like Gradual Multi Agent Q-learning is the proposed new approach of Q-learning for multi-agent systems. The human-like gradual learning has already been explained in the above paragraphs. The human-like gradual Q-learning for various multi-agent systems will be discussed in the following paragraphs. This is simpler than any other multi-agent Q-learning. As shown in fig. 2, the system interacts with the environment with the help of a 'Co-ordinator'. It is one the main parts of HuMAQ.

The system has 'N' numbers of agents responsible for different states generated by the sensors and by some internal states. For a simple system, each agent can take care of 2 states of the robot. For a more complex system, each agent can take care of n states. On the basis of the different states, each agent chooses different actions and sends to the Co-ordinator. This co-ordinator arranges the agents according to the priority as shown in fig. 3. For example if there are four agents; hunger, goal-seeking, obstacle-avoidance and line-following; they can be arranged as hunger, obstacle-avoidance, goal-seeking and line-following according to the priority. Hunger should have the highest priority, as no system can move or work without energy.

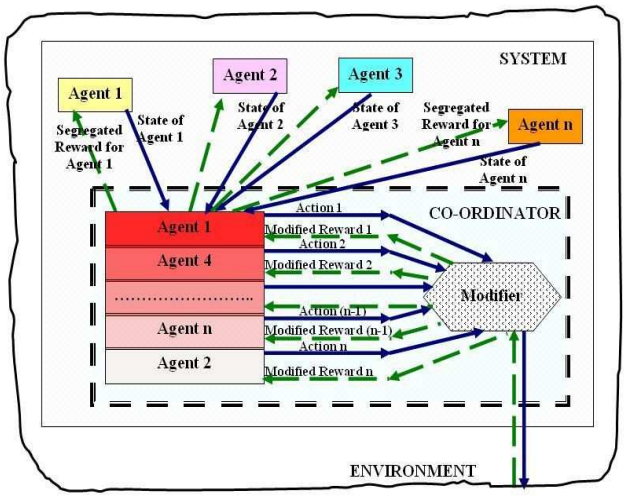

Fig. 3. The Proposed Generalized Co-ordinator for HuMAQ. The main part of the co-ordinator is the modifier. It modifies the actions for different agents depending upon the priority and distributes the reward accordingly

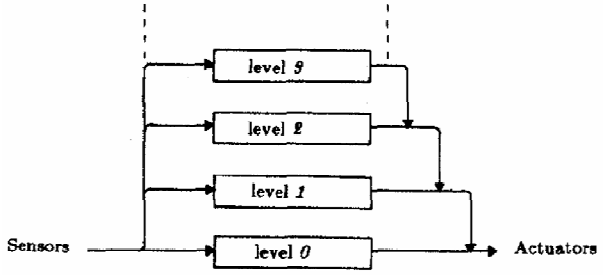

Fig. 4. Subsumption Architecture is a layered based control system for robots as proposed by Rodney Brooks. The top layers have higher priority over the bottom layers.

The next priority is of the obstacle-avoidance agent, as obstacle avoidance is the second most important issue after the power supply for real time explorations. The last two agents according to the priority are goal-seeking and line-following respectively, as goal-seeking is the main objective of any autonomous field exploration rather than the line- following. This concept of priority is based on Brook's Subsumption Architecture. As shown in fig. 4, this is a layer-based control for robots and distributed and parallel methods to connect sensors and actuators in robots. Each parallel layer (layer 2, layer 1 and layer 0) is made up of simple processors, called Augmented Finite State Machines (FSM). The most important aspects of FSMs are that

outputs are simple function of inputs and local variables; inputs can be suppressed and outputs can be inhibitated.

Co-ordinator has an important sub-part known as modifier. The modifier refines the actions proposed by different agents depending upon their priorities. For example, if the goal-seeking agent has directed the robot to move in forward direction, but the obstacle-avoidance agent has detected obstacle in the front, the modifier searches the second point from where the goal is nearer and refines the action as move forward in left or move forward in right. The modifier tries to find out a common intersecting area (as shown in fig. 5) where the states from most of the different agents are available and then refines the action from the descending list of states from that common space accordingly. It is not mandatory that all the states from all the agents are present as in any instance of time all the agents may not be active. With the increase in number of agents, the complexity of the co-ordinator and modifier also increases.

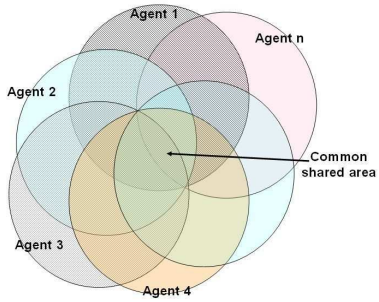

Fig. 5. The common shared area by all the agents is chosen by the modifier for consideration.

The refined action is performed by the actuators and the obtained reward is again sent to the modifier to distribute them as per the priority of the agents only to those, which were active for obtaining the particular reward. So, instead of a single reward as in the case of Q-learning, here a distributed and gradually reducing weightage system has been used. Such a variable weightage system has been used to accommodate the difference in priority of the agents. For example, if there are four agents and the total reward obtained is R for any instance of time, when all the four agents were responsible for a refined action, it can be distributed as mentioned in eqn. 4 below.

$$R = \omega_1 R_1 + \omega_2 R_2 + \omega_3 R_3 + \omega_4 R_4 \quad (4)$$

Where $\omega_1 > \omega_2 > \omega_3 > \omega_4$; $\omega_1 + \omega_2 + \omega_3 + \omega_4 = 1$; $\omega_1, \omega_2, \omega_3, \omega_4$ are the distributed weightage for rewards for agent 1 (highest priority), agent 2, agent 3 and agent 4 (low priority) respectively. R_1, R_2, R_3 and R_4 are the individual rewards for agent 1, agent 2, agent 3 and agent 4 respectively obtained directly due to system-environment interactions. With these separate rewards $\omega_i R_i (i \in 1,2,3,4)$, the separate Q-tables for different agents update themselves gradually. After a long run in any field exploration, if the system needs to be recharged or powered off for any reason, the final Q-table at that instance is stored and will be used as initial table for next run onwards. More details about this have been given in the following example.

C. Simplified Methodology for Field Exploration

It has been noted that even if only a few sensors are used, the numbers of possible states become large. In an indoor exploration (goal seeking) with the help of light sensor, ultrasonic sensor, compass and battery-level detector (four different agents), nos. of states possible are in the order of 10^8or more. It may be very difficult to implement such a system in real time robots as it will need huge computational power and complexity. To simplify this model only three very necessary sensors and three related agents have been used in real experiments. Also several assumptions have been made and as a result the total numbers of states have reduced to very minimum (in the order of 10^3).

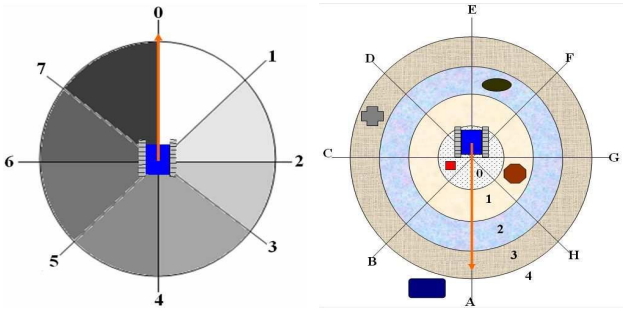

Fig. 6. (a) The numbering of the sectors is done in the clockwise direction with reference to the front direction of the robot. The numbers of the sectors are considered for denoting the brightness of the environment around the robot. (b) The surroundings of the robot can be differentiated as near, near-far, far, farther and farthest depending upon its distance. All these circles can again be divided into eight sectors. Obstacles with different colours and shapes have been found at different distances and different sectors.

Sensors are used to get the complete information of all the disturbances of the environment around a robotic system. In ideal case any sensor should have 360° views of the environment. Here the sensors have been mounted on a rotating head to take the readings around the robot (360° view). Instead of continuous readin g a sector wise reading is preferred. Continuous reading will show gradual change in the reading of light; where as the sector wise reading will depict sudden change from sector to sector. Smaller division will lead to more numbers of sectors and consequently more numbers of sectors will show only a little difference in analogue values of the readings and the sensor will take longer

time to read the data. But in some cases (in a dynamic environment), this delay may cause a problem. Similarly, for a few divisions, only a numbers of sectors with larger area will be generated and such large sectors will make a huge deviation in the trajectory of the robot and this may lead the robot to wrong direction and the time for error correction will make a cumulative effect on the mission time.

For a goal-directed field exploration, the minimum sensors to be used are (1) for monitoring the voltage of the battery (2) for detecting the goal (3) for avoiding the obstacles. In this case three different agents have been used for describing the states of these sensors as Hunger, Goal-seeking and Obstacle-avoidance respectively for a successful exploration.

1) *Agent – Hunger:* As already described, the agent hunger is responsible for the monitoring the battery-voltage level and denotes its sub-states as above the threshold voltage (can be denoted by '0') or below the threshold voltage ('1'). The probable actions for this agent shut-down the system and do not shut-down.

2) Agent – Light-seeking: Considering all the aspects of both smaller and larger sectors, here the (imaginary) circle around the robot is divided into 8 equal sectors each making an angle of 45° at the centre. The light sensor takes reading only on boundary line (45° apart from each other) and differentiates the sectors according to the intensity of the light and the boundary line of the sectors are assigned values from 0 to 7 in the clockwise direction with reference to the front direction of the robot (shown with red coloured arrow line in fig. 6(a)). In actual case the arrangements of bright and dark sectors do not occur regularly, there may be repetition and irregular arrangements.

From the above convention, it is clear that the brightest sector can have 8 values (0 to 7). For example, say the brightest zone is the first sector i.e. with value 0. For this single value, the next brighter zone can have 8 values. So, for these two sectors together, for the single value of the first sector, 1×8 possible combinations can occur. Again the next bright sector can have 8 values. For these three sectors 1×8×8 (= 8^2=64) values are possible, for a single value of the first sector. For all the8 values of the first sector, there can be 8×8×8 (=8^3) combinations for the three sectors. For 8 sectors total 8^8 numbers of combinations are possible. This refers to 16777216 numbers of possible states of the robot. But such a large combination of states will lead to computational complexity and require huge memory power and operational time.

TABLE II
STATE TABLE FOR THE GOAL-SEEKING AGENT

No. of the maximum intensity	No. of the second maximum	No. of the third maximum	Repetition
grid	**grid**	**grid**	
Percept ID 1	**Percept ID 2**	**Percept ID 3**	**Percept ID 4**
0	1	2	0

To overcome the above difficulties, instead of considering all the 8 sectors, three sectors with consecutive maximum brightness values are considered. So, total 8^3 (8×8×8) i.e. 512 numbers of states are possible instead of 8^8. As the goal of the exploration is to search the brightest part of the environment, constant movement is essential for the robot. It may also happen that the robot is stationary and as a result the reading of a particular sector is constant for the last few couple of minutes. This is defined as another percept and it can be denoted as 'whether the system has five repeated readings or not'. If it is 'Yes', the value 1 is assigned and for 'No', 0 is assigned. So, in total 1024 (512×2) numbers of states are possible. The above table (table II) shows that the state of the robot is denoted by a 4 digit number. Here 4 nos. of percepts are considered having ID 1, 2, 3, 4.

This entire phenomenon is taken care of by the goal-seeking agent (agent 1). The detail schematic diagram for only the goal-seeking agent is given in fig. 7.

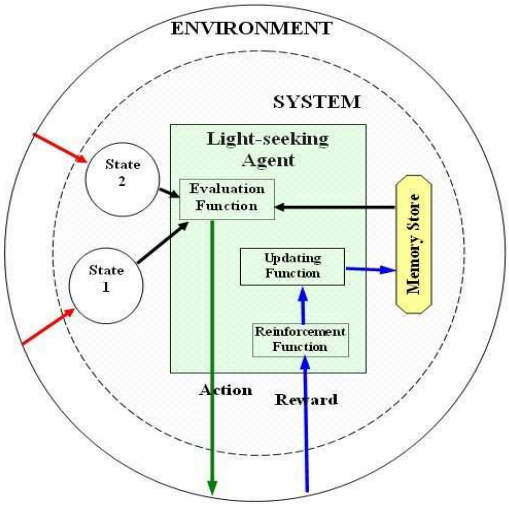

Fig. 7. The detail schematic diagram for the operation of the light-seeking agent (agent 1) shows that not only the system (robot) and the environment are considered, but also the memory of the robot is associated for determining the states.

The actions for this agent are given in table III. These actions are in terms of rotation of the robot along the sectors. As eight sectors have been considered for measuring the sensor values of the environment, there should also be eight rotations starting from 0° to 315° in steps of 45° as shown in table III. If the brightest zone is

sector 0, (i.e. along the forward direction of the robot at current position) the robot will not rotate. But if the brightest zone is sector 7, the robot will rotate through an angle of 315° (i.e. 7 × 45°) clockwise. The goal - seeking agent chooses the action from the Q-table and sends to the co-ordinator.

TABLE III
ACTION TABLE FOR GOAL-SEEKING AGENT

Actions	Action ID
No rotation	0
Clockwise rotation through **45°**	1
Clockwise rotation through **90°**	2
Clockwise rotation through **135°**	3
Clockwise rotation through **180°**	4
Clockwise rotation through **225°**	5
Clockwise rotation through **270°**	6
Clockwise rotation through **315°**	7

1) *Agent – Obstacle-avoidance:* The ultrasonic sensor detects the obstacles and measures the distance. The obstacles only at the plane of the ultrasonic sensor are detected by the sensor. The surroundings of the robot can be referred as near, near-far, far, farther and farthest according to the distance and they can be denoted by circles (from 0 to 4) as shown in fig. 6(b). The approximate radii for these circles are given in table IV.

TABLE IV
DISTANCE TABLE FOR LOCATING OBSTACLES FOR OBSTACLE-AVOIDANCE AGENT

Relative position	Near	Near – far	Far	Farther	Farthest
Approximate distance (cm)	≤ 50	50 - 100	100 - 150	150 - 200	> 200
Number of the zone	0	1	2	3	4

Each individual circle surrounding the robot (circles around it) is again divided in 8 sectors (A to H). Total nos. of states for obstacles-avoiding agent can be found out in the similar manner as done in the case of goal-seeking agent. Suppose an obstacle is detected inside the first circle (no. 0) and in the second sector (no. B) as shown by a red square in fig. 6(b). So, for this single obstacle, there may be 5 possibilities (as there are only 5 circles) of an obstacle to be present in the next sectors i.e. first, second, third and fourth circle. This is to be noted that it is immaterial whether more objects are detected behind the first obstacle in the same sector. In such cases only the first obstacle (nearest to the centre of the circles) is considered. So together, 1 × 5 combinations are possible. Again, if the third sector is considered, total 1×5×5 (or 5^2) combinations can be obtained. For all the sectors of the different circles, in total 5^8 i.e. 390625 combinations (i.e. states) are available. But as in the earlier case, it is not possible to handle such large amount of data which require a lot of computational power, memory space and processing time.

For the simplicity, rather only those sectors of the circles are considered, where the brightness is maximum, second maximum and third maximum. Thus the total nos. of states reduces to 5^3 i.e. 125 nos. instead of 5^8 combinations. The robot should also move continuously to avoid trap. So, to avoid traps repeated readings of the robots should be avoided. This is denoted by another state: 'Repeated reading?'- Yes or No which is referred by 1 and 0. So, here 2 combinations are possible and in total 125 × 2 (=250) nos. states can be obtained. In this case the state table will also consist of 4 digits as given in table V. The state IDs along with their description is given in the table below.

The Avoid-obstacle agent locates the obstacles and finds out their position. This agent works independently with out any intervention by other agents. The action for this agent is given in table VI. Here all the three agents work independently and separately. But they are sharing information as the goal-seeking agent passes the information of three maximum brightness zones to the obstacle-avoidance agent.

Table V

The state Table for the Obstacle-avoidance Agent

Obstacle in the Maximum Intense Zone	Obstacle in the Second Maximum Intense Zone	Obstacle in the Third Maximum Intense Zone	Repetition
Percept ID 1	**Percept ID 2**	**Percept ID 3**	**Percept ID 4**
0	1	2	0

Table VI

Action Table for Obstacle-avoidance Agent

Position of obstacles	Within 1st circle	Between 1st and 2nd circle	Between 2nd and 3rd circle	Between 3rd and 4th circle	Outside 4th circle
Speed (RPM)	34	67	84	100	117
Action ID	0	1	2	3	4

1) Co-ordinator and the Modifier: All the sub-states and the recommended actions for different agents are forwarded to co-ordinator for selecting the refined action. The modifier chooses the refined actions against the above simplified states from the initial or updated Q-table based on the Q-values.

All the three agents are sending data (sub-states and action) simultaneously to the Co-ordinator. As the agent Hunger, is of highest priority, the co-ordinator sorts out this agent first and forward its recommended action and sub-state to the modifier. If the recommended action is 'shut-down system', the same is passed for action. No other command by other agents will be considered. But if the action is 'do not shut down', the modifier looks for the next priority agent. The next priority agent is the Goal-seeking agent. The agent gathers the data (brightness) from the surroundings and arranges only three of them (numbers of sectors with different brightness) in descending order starting with the maximum. Suppose the sub-states for such a case is '2 – 3 – 1'. The action related to the maximum brightness is rotation through an angle (= number of the sector × 45°) in the clockwise direction (as the reading has been taken in a step of 45° in the clockwise direction). Here it will be rotation through 90° (2 × 45°). The sub-sta tes and the action are passed to modifier for further action. Obstacle-avoidance agent is the agent with last priority. This agent gathers the data about the presence of obstacles in the sectors and circles (1st, 2nd, 3rd and 4th) and compares them with the sectors of first, second and third maximum brightness. Then the agent passes the sub-states and action to the Co-ordinator for refinement. Here for 5 different zones (within 1st , 2nd , 3rd and 4th circle and outside 4th circle) and 3 different brightness regions, total 215 combinations are possible for presence ('1') or absence ('0') of obstacles. The modifier chooses the action according to following rules.

Rule - I: If there is an obstacle within the first circle of the brightest zone, go to second bright zone. If there is an obstacle also within the first circle of the second bright zone, go to the third bright zone. If there is an obstacle with in the first circle of the third bright zone, the system may stand still.

Rule - II: If the obstacle is not within the first circle, but within second or third or fourth circle of the considered bright zone, the system will use modified speed as given in table VI. In this regard a point may be noted that if there is an obstacle within the first circle of the brightest zone; another obstacle within the second circle (more specifically between first and second circle) of the second bright zone and no obstacle in the third bright zone, the modifier will make the system move along the second bright zone with modified speed.

The reward obtained due to the past action is updated in the Q-table for respective agents. Here two cases may happen.

Case-I: When the agent hunger detects that the voltage level is below the predefined threshold limit, the reward will be totally updated to the Q-table of the agent hunger, as this agent solely defines the action.

Case-II: When the agent hunger detects that the voltage level is above the predefined threshold limit, the reward is distributed with reducing weightage as mentioned in equation 2.

Here as only three agents are active, goal-seeking, obstacle-avoidance and direction-correction, the rewards are distributed with the weightages 0.6, 0.3 and0.1 respectively. The reward for goal-seeking is calculated as:

$$[(L_{\max})_i - (L_{\max})_{i-1}] \quad \text{..... (3a)}$$

Where $(L_{\max})_{i-1}$ = maximum light value of the previous state $(i-1)$ in the direction of motion of the robot and $(L_{\max})_i$ = maximum light value in the (i) current state for that same direction. Similar policy is also adapted for obstacle-avoidance agent as mentioned in eqn. 3(b).

$$[(D_{\max})_i] \quad \text{..... (3b)}$$

Where $(D_{\max})_i$ = maximum distance of the obstacle (if present or '255' if not present. 255 is the maximum range of the ultrasonic sensor) in the same direction in

which the robot has moved to reach the (i) current state.

For no repetition in any of the above mentioned agents, a positive scalar reward of magnitude '10' or '100' and for repetition a negative reward (i.e. punishment) of '-20' or '-200' have been used. The punishment should be always higher than the reward so as to stop selecting any wrong policy. The high value of punishment will completely abandon the associated action. These rewards multiplied with the weightage factors are updated in the respective Q-tables of different agents.

V. EXPERIMENTAL RESULTS AND DISCUSSIONS

A.Experiment

Different experiments in the field of Behavior-based robotics, Reinforcement learning has been carried out in different environments using different robotic systems. Initially it was a challenge to identify the right Behavior-based architecture for implementation. For this purpose two most popular architectures (Subsumption architecture and Motor-schema theory) have been tested in simulated environment. Using the identified architecture, the next series of experiments have been carried out in simulated environment (fig 8(a)), indoor environment (fig 8(b)) and different outdoor terrains (fig 8(c)-(f)). Most of these experiments include only three agents: hunger, goal-seeking and the obstacle-avoidance using the battery-level detector, light sensor and ultrasonic sensor respectively. The data of the experiments have been saved on the robot itself and later downloaded for further processing.

The experiments with HuMAQ are carried out in five trial runs on different outdoor terrains each with five sets. The first set of each trial run uses a randomly initialized Q-table and from second run onwards, final updated Q-table of the previous set is used as the initial Q-table of the next set.

B.Experimental Systems

In these sets of experiments four different sets of robots have been used. Initially the experiments have been carried out with indigenously developed three different robots: ARBIB (Autonomous Robot Based on Intelligent Behaviors) – I, II and III. The testing for HuMAQ has been mostly carried out on LEGO Mindstorm NXT due to its simple and perfect analog sensors. The above figures [9(a) – (d)] show the different robots used during various experiments.

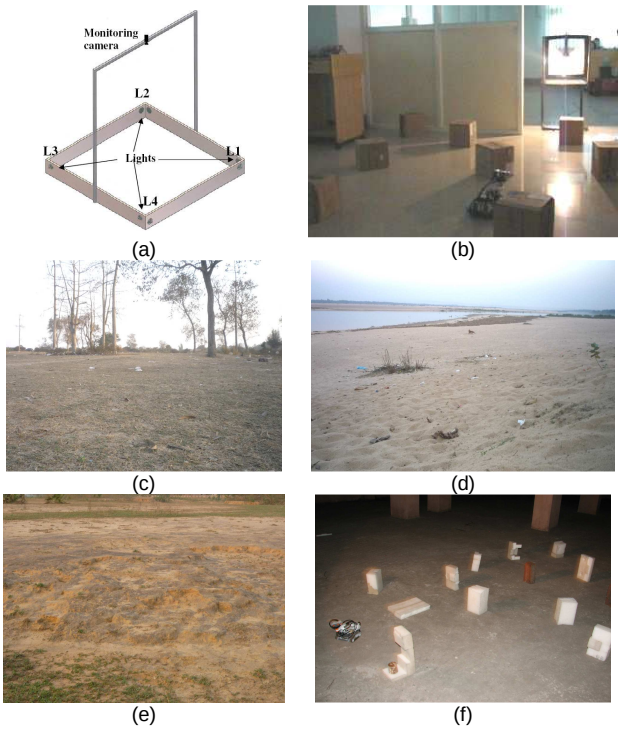

Fig. 8. Environments where different experiments have been carried out (a) Simulated environment (b) Indoor environment (c) Outdoor terrain – Plain grassland (d) Outdoor terrain – Loose sand (e) Outdoor terrain – Laterite tableland (f) Outdoor terrain- Roof of the laboratory during night

Fig. 9. Different Robotic Systems used in the Experiments (a) ARBIB-I (b) ARBIB-II (c) ARBIB-III (d) LEGO Mindstorm [courtesy: LEGO Group]

Items	Set A	Set B	Set C	Set D	Set E
Value Increased	42	60	71	78	82
Value Decreased	19	19	19	19	19
Total Change	***61***	***79***	***90***	***97***	***101***

Table IX

Cumulative Change of Q-values (compared to intial value) in the Q-table for the Obstacle-avoidance Agent (Ultrasonic sensor) in Indoor Environment

Items	Set A	Set B	Set C	Set D	Set E
Value Increased	16	31	36	41	44
Value Decreased	9	9	9	9	9
Total Change	***25***	***40***	***45***	***50***	***53***

Table X

C.Results and Discussions

After the successful completion of the exploration in indoor environment using HuMAQ, the data are downloaded for analysis. The first set (Set A) of the trial run is done with a randomly generated Q-table. In this set, 54 nos. of updates are performed to reach the goal. The second set also took 54 nos. of updates to reach its goal, but started with the final table of set A as initial table. The nos. of updates for other sets of the same trial run and the approximate time to reach the goal has been given in table VII. When these numbers of updates (or the approximated time) are plotted, produces a graph as shown in fig. 10(a) which is gradually decaying down. This gradual decrease in nos. of updates or approximated time indicates that learning is occurring in real time. If the experiment is carried out for few more sets, the curve will become flat. It means that the learning has reaches the optimality.

Table VIII and IX show the cumulative change of Q-values in the Q-table with respect to its initial values for goal-seeking (using light sensor) and obstacle-avoidance (using ultrasonic sensor) agents respectively. The different between two consecutive columns (i.e. sets) gives the particular change of the Q-values occurred in the later. If these particular values for different columns (sets) are compared, it will also show a decreasing tendency and this proves the efficiency of the learning.

Table VII

Numbers of Updates and Approximate Time Required (Sec) for Reaching the Goal in an Indoor Environment using HuMAQ

	Set A	Set B	Set C	Set D	Set E
Nos. of Updates	**57**	**56**	**48**	**38**	**34**
Time Required (Sec)	**1141**	**1122**	**964**	**762**	**685**

Table VIII

Cumulative Change of Q-values (compared to intial value) in the Q-table for the Goal-seeking Agent (Light sensor) in Indoor Environment

Durations (in sec) for reaching the goal

Types of Terrains	Set A	Set B	Set C	Set D	Set E
Plain Grass land	1382	1203	784	904	781
Sandy river bank	1323	1081	1022	904	900
Hard concrete floor	1201	1025	845	802	761
Laterite table land	902	783	722	601	600
Hard concrete floor at night	1261	1203	904	843	842

Table XI

Cumulative Change of Q-values (compared to intial value) of the various state-action pairs for the Goal-seeking Agent (Light sensor)

Types of Terrains	Items	Set A	Set B	Set C	Set D	Set E
Plain Grass land	*Value Increased*	46	56	62	65	66
	Value Decreased	19	19	19	19	19
	Total Change	***65***	***75***	***81***	***84***	***85***
Sandy river bank	*Value Increased*	35	46	50	52	54
	Value Decreased	20	20	20	20	20
	Total Change	**55**	**66**	**70**	**72**	**74**
Hard concrete floor	*Value Increased*	43	52	60	70	79
	Value Decreased	19	19	19	19	19
	Total Change	***62***	***71***	***79***	***89***	***98***
Laterite table land	*Value Increased*	30	36	42	47	48
	Value Decreased	26	26	26	26	26
	Total Change	***56***	***62***	***68***	***73***	***74***
Hard concrete floor at night	*Value Increased*	47	57	59	64	66
	Value Decreased	17	17	17	17	17
	Total	***64***	***74***	***76***	***81***	***83***

Types of Terrains	Items	Set A	Set B	Set C	Set D	Set E
	Change					

Table XII

Cumulative Change of Q-values (compared to intial value) of the various state-action pairs for the Obstacle-avoidance Agent (Ultrasonic sensor)

Types of Terrains	Items	Set A	Set B	Set C	Set D	Set E
Plain Grass land	*Value Increased*	18	26	30	31	33
	Value Decreased	6	6	6	6	6
	Total Change	***24***	***32***	***36***	***37***	***39***
Sandy river bank	*Value Increased*	15	24	28	31	33
	Value Decreased	5	5	5	5	5
	Total Change	**20**	**29**	**33**	**36**	**38**
Hard concrete floor	*Value Increased*	13	21	25	26	28
	Value Decreased	2	2	2	2	2
	Total Change	***15***	***23***	***27***	***28***	***30***
Laterite table land	*Value Increased*	11	13	15	19	22
	Value Decreased	5	5	5	5	5
	Total Change	***16***	***18***	***20***	***24***	***27***
Hard concrete floor at night	*Value Increased*	12	17	19	21	22
	Value Decreased	9	9	9	9	9
	Total Change	***21***	***26***	***28***	***30***	***31***

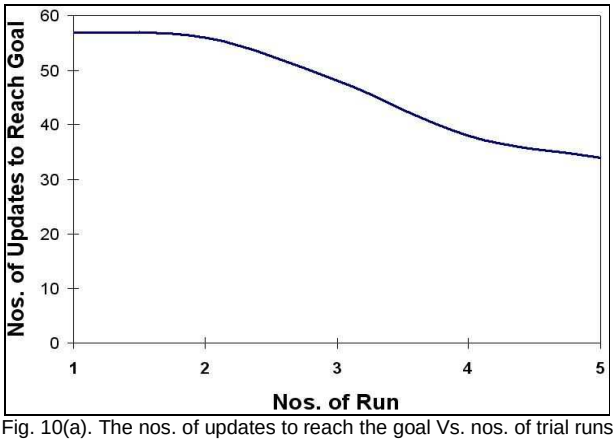

Fig. 10(a). The nos. of updates to reach the goal Vs. nos. of trial runs shows a gradually reducing nature which in fact supports the actual learning using HuMAQ in indoor environment.

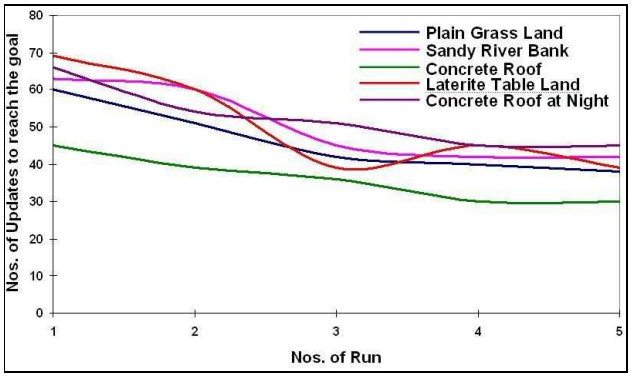

Fig. 10(b). The time to reach the goal Vs. run nos. shows a good acceptability of HuMAQ for autonomous exploration in outdoor terrains. As expected, the initial time was higher than the later.

In similar manner, the different data recorded during the outdoor field explorations and the extracted data/ information generated thereafter have been given in the above tables/ sections. The durations for reaching the goals (calculated thereafter) different sets of the different trial runs have been given in table X.

The cumulative change of Q-values in the Q-table with reference to the initial values for both goal-seeking and obstacle-avoidance agents have been given in table XI and XII respectively.

One important issue for any learning algorithm/ theory is that if learning is applied in the same field for same objectives repeatedly, the learning time/objective fulfilment time should reduce. This point has also been fulfilled in the case of application of HuMAQ for autonomous explorations. It is clear from table X that the time for reaching the goal from the same starting point, are gradually reducing in nature. For example, if the experiment over the plain grass land is considered, the initial nos. of updates to reach the goal is 66 with randomly generated Q-table and the final (set E) nos. of updates to reach the goal is 45 using the concept of gradual learning. For all other intermediate sets, the update-counts are lying between 66 and 45.

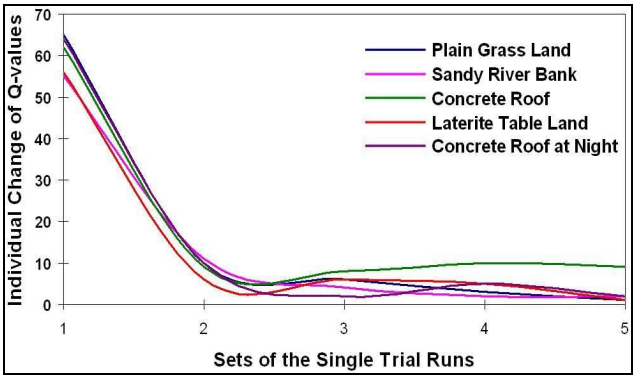

Fig. 11. The individual change of Q-values of the goal – seeking agent (light sensor) for different sets of the different trial runs proves the convergence of the learning.

D. Performance of the Learning Algorithm

As described in [25], 'optimality is usually an asymptotic result and so convergence speed is an ill-defined measure'. As optimality may not be well defined, more practical measure is speed of convergence to near – optimality. This indicates that someone should define how near the optimality is sufficient. The speed of convergence or the rate of convergence can be defined [31] as follows. If a sequence of numbers ($a_1, a_2, a_3,$ ……. a_k) is considered and this sequence converges to the number L, it can be said that this sequence converges linearly to L, if there exists a number, μ =(0, 1) such that

$$\lim_{k\to\infty} \frac{|a_{k+1} - L|}{|a_k - L|} = \mu$$

This μ is known as the speed or rate of convergence. If μ =0, it is said the sequence converges linearly and if μ =1, the sequence converges sub-linearly.

If the updates of the trial runs for explorations in outdoor environment are considered as sequence of numbers, for example, for the first trial run (experiment on plain grass land) the updates are 69 (set A), 60 (set B), 39 (set C), 45 (set D), 39 (set E) and if the lowest of all the updates of the five sets of a trial run is considered as optimal one or near optimality, the speed or rate of convergence is calculated as shown below in table XIII. In the above mentioned first trial run the optimum value is 39 (i.e. L) and all the calculations in absolute values are done with respect to this value. Different optimal values for different fields are set as the experiments have been carried out in different environmental conditions.

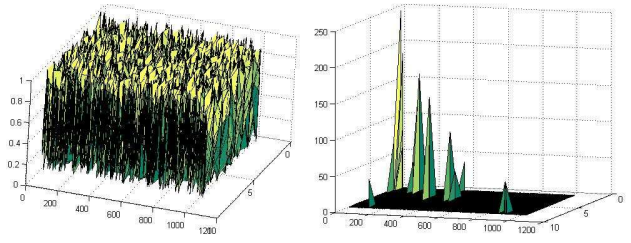

Fig. 12(a). Initial Q-table for light sensor during testing on plain grass land (b) Final Q-table for light sensor during testing on plain grass land

Table XIII

Speed of Convergence for the Updates for Outdoor Exploration

Types of Terrains	Set A	Set B	Set C	Set D	Set E
Plain grass land	0.7	0	-	0	-
Sandy river bank	0.4	0.7	0	-	-
Hard concrete floor	0.6	0.3	0.5	0	-
Laterite table land	0.6	0.7	0	-	-
Hard concrete floor at night	0.9	0.2	0	-	-

The speed of convergence lies between 0 and 1 that means this is linear in nature. The cell is left blank where the value is undefined. The higher values of speed of convergence refer to fast reaching of the optimality and the lower values lead to slow reaching. However a medium speed of convergence is preferred as both higher and lower values may be misleading [25].

E. Comparison with Other Reinforcement Learning Methods

Dynamic programming and Monte Carlo Methods are the two well known methods under reinforcement learning. Dynamic programming refers to a collection of algorithms that can be used to compute optimal policies given a perfect model of the environment as a Markov decision process [1]. Monte Carlo methods are ways of solving the reinforcement learning problem based on averaging sample returns [1]. Experiments have been carried out using Dynamic Programming and Monte Carlo methods in the indoor environment with same environmental and experimental parameters. The results obtained are plotted in fig. 13 (a) and (b). Both the graphs clearly show (even if only 4 iterations are considered for comparison in all cases) that they do not follow similar pattern as in the case of HuMAQ and thus could not provide efficient learning. In both cases the initial learning time is less than the final learning time. Human-like gradual learning provides better result than these methods.

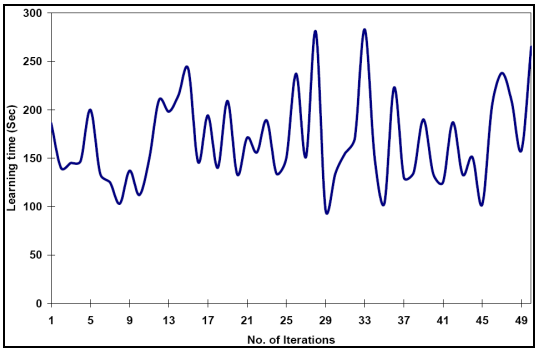

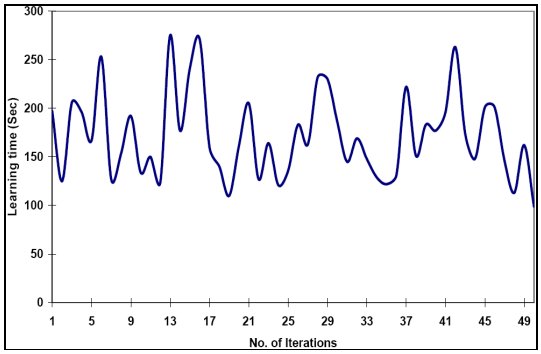

Fig. 13. Comparison with other Reinforcement Learning Methods: Curves for learning time vs. no. of iterations to reach the goal using (a) On-policy Monte Carlo Method [Top] (b) Dynamic Programming

VI. CONCLUSION

The behavior-based robotics has opened up a new field of robotics which uses the Sense →Act paradigm for achieving the low-level intelligence easily. Four different behavior-based architectures are popular, out of which only two (Subsumption architecture and the Motor-schema Theory) have been tested to implement here.

The reinforcement learning is a suitable machine learning approach for implementing in mobile robots and this is a direct system-environment interaction based on reward/ punishment policy. Q-learning a sub-issue of reinforcement learning uses delayed reward/punishment for the previous action. It uses a state-action mapping table based on the different conditions of the sensors (states) and commands to the actuators (action). Agent is a software entity which performs an assigned task independently. In most cases Q-learning uses single agent to perform all the tasks for learning. Use of multiagent is preferred to handle with large numbers of sensors and therefore large numbers of state-action mapping.

As revealed from various literatures, human learning is cumulative and gradual in nature and as time passes the learning time for the same topic/ subject reduces. This concept of gradual learning can be incorporated with the multiagent Q-learning to get a better performance in outdoor terrain explorations by mobile robots.

Here a new approach of multiagent reinforcement learning has been proposed using the concept of Subsumption architecture, a well-known behavior-based architecture, and the gradual learning technique for autonomous exploration. It uses different agent on single system, not different agents on different systems. The testing of HuMAQ in different terrains, different static and partial dynamic conditions reveal the acceptance of the algorithm for autonomous explorations by mobile robots. Also the measurement of the performance of the learning algorithm has been done from the proof of convergence.

ACKNOWLEDGMENT

This work has been carried out as a part of SIP-24, an 11th Five Year Project funded by CSIR, Govt. of India.

Authors also thank CMERI personals who have directly and indirectly helped to complete this project. It will be injustice if the constant help and effort made by Mr. Amit Mandal, research scholar in this project, and Mr. A. Mahapatra, scientist, CMERI is not acknowledged.

REFERENCES

R. S. Sutton and A. Barto, “Reinforcement Learning: An Introduction”, MIT Press, New York, 1998.

M. Wunder, M. L. Littman, M. Babes, “Classes of multiagent Q-learning dynamics with e-greedy exploration”. Proc. of International Conference on Machine Learning (ICML 2010), Haifa, Israel, Omnipress, pp. 1167-1174, June 2010.

Liviu Panait and Sean Luke, “Cooperative Multi-Agent Learning: The State of the Art”, Journal of Autonomous Agents and Multi-agent Systems, Vol. 11(3), pp. 387 – 434, 2005.

Adrian K. Agogino and Kagan Tummer, “Quicker Q-Learning in Multi-Agent Systems,” [Online], www.citeseerx.ist.psu.edu/ viewdoc/download?doi=10.1.1.133.3323

L. Busoniu, R. Babuska, and B.D. Schutter, "Multi-Agent Reinforcement Learning: A Survey", Proc. of 9th International Conference on Control, Automation, Robotics and Vision, Singapore, pp.527- 5326, December 2006.

Michael L. Littman, “Friend-or-Foe Q-learning in General-sum Games,” Proceedings of the Eighteenth International Conference on Machine Learning, pp. 322-328, USA, June-July 2001.

Reinaldo A. C. Bianchi, Ramon López de Mántaras. “Case-Based Multiagent Reinforcement Learning: Cases as Heuristics for Selection of Actions”. In Proceedings of 19th European Conference on Artificial Intelligence 2010, Portugal, pp. 355-360, August 2010.

T. Fujii, Y. Arai , H. Asama, I. Endo, “Multilayered Rienforcement Learning For Complicated collision Avoidance problems,” Proceedings of IEEE International Conference on Robotics & Automation, Belgium, Vol. 3, pp. 2186-2191, May 1998.

A. Merke, M. A. Riedmiller, "Karlsruhe Brainstormers – A Reinforcement Learning Approach to RoboticSoccer", In Proceedings of RoboCup-2001, USA, pp. 435- 440, August 2001.

Jong- Hawn Kim and Prahlad Vadakkepat, “Multiagent Systems: A survey from the Robot Soccer Perspective”, Journal of Intelligent Automation and Soft computing, Vol. 6, No. 1, pp. 3-17,TSI Press, USA, 2000.

Kui-Hong Park, Yong-Jae Kim and Jong-Hwan Kim, “Modular Q-learning based multi-agent cooperation for robot soccer”, Journal of Robotics and Autonomous Systems, Volume 35, Pp.109-12231, May 2001.

Michael L. Littman,” Markov Games as a Framework for Multi-agent Reinforcement Learning,” Proceedings of the Eleventh International Conference on Machine Learning, Volume: 157, Publisher: Morgan Kaufmann, Pages: 157-163, 1994.

William D. Smart and Leslie Pack Kaelbling, "Effective Reinforcement Learning for Mobile Robots," Proc. of the IEEE International Conference on Robotics and Automation, Washington DC, Vol. 4, pp. 3404 – 3410, May 2002.

Georgios Chalkiadakis, “Multiagent Reinforcement Learning: Stochastic Games with Multiple Learning Players”, PhD Thesis, Department of Computer Science, University of Toronto, 2003.

Rodney A. Brooks, “Cambrian Intelligence the Early History of the New AI”, The MIT Press, 1999.
R. Brooks, “Intelligence without reason”, Proc. of the Conference of International Joint Conference on Artificial Intelligence (IJCAI), 1991.
Rodney A. Brooks and Stein L. Andrea, “Building Brains for Bodies”, A.I. Memo No. 1439, 1993.
R. Brooks, “A Robust Layered Control System for a Mobile Robot”, IEEE Journal of Robotics & Automation, Vol. 2, No.1, Page 14-23, 1986.
P. Maes, “The Dynamics of Action Selection”, Proceedings of the International Joint Conference on Artificial Intelligence, pp. 991-997, 1989.
M. Arbib, “Schema Theory”, In Encyclopedia of Artificial Intelligence, 2nd Edition, Vol. 2, pp 1427-1443, Jhon Wiley and Sons., New York, 1992.
Ronald C. Arkin, “Motor Schema — Based Mobile Robot Navigation”, The International Journal of Robotics Research, Vol. 8, No. 4, 92-112, 1989
Ronald C. Arkin, “Behavior-Based Robotics”, The MIT Press, 1998.
R. C. Arkin, “Integrating Behavioral, Perceptual, and World Knowledge in Reactive Navigation”, Journal of Robotics and Autonomous Systems, Page 105-122, 1990.
L. Steels, “A Case study in the behavior-oriented design of autonomous agents”, Proc. of 3rd International Conference on Simulation of Adaptive Behavior, The MIT Press/ Bradford Books, 1994
L. P. Kaelbling, M. L. Littman and A. W. Moore, “Reinforcement learning: a survey,” Journal of Artificial Intelligence Research, Vol. 4, pp. 237 – 285, 1996.
C. J. C. H. Watkins, Learning from Delayed Rewards, PhD thesis submitted to King’s College, Cambridge, UK, 1989.
C. J. C. H. Watkins and P. Dayan, “Technical note: Q-learning,” Machine Learning: Special Issue on Reinforcement Learning, Vol. 8 (3-4), pp.279 – 292, 1992.
Y. Dahmani and A. Benyettou, “Seek of an Optimal Way by Q-learning”, Journal of Computer Science, Vol. 1 (1), pp. 28 – 30. 2005.
H. Nwana, “Software Agents: An Overview”, The Knowledge Engineering Review, 11 (3), 205-244, 1996.
S. Vosniadou, “How Children Learn,” International Academy of Education, www.ibe.unesco.org/publications/EducationalPracticesSeriesPdf/prac07e.pdf
M. Schatzman, “Numerical analysis: A Mathematical Introduction”, Clarendon Press, Oxford, 2002.

INTERNATIONAL JOURNAL OF INNOVATIVE TECHNOLOGY & CREATIVE ENGINEERING (ISSN:2045-8711)
VOL.1 NO.7 JULY 2011

A Hybrid Prediction System Using Rough Sets and Artificial Neural Networks

M. Durairaj [#1], K. Meena [*2]

[#] *Assistant Professor, Department of Computer Science and Engineering, Bharathidasan University, Tamilnadu, India*

[1] durairaj_m@csbdu.in

[*] *Vice-chancellor, Bharathidasan University, Tamilnadu, India*

***Abstract*— This paper illustrates a hybrid prediction system consists of Rough Set Theory (RST) and Artificial Neural Network (ANN) for processing medical data. In the process of developing a new data mining technique and software to aid efficient solutions for medical data analysis, we propose a hybrid tool that incorporates RST and ANN to make efficient data analysis and suggestive predictions. In the experiments, we used spermatological data set for predicting quality of animal semen. The data set used in the experiments is subjected to quantize and normalize, and use this as a reflection of the internal system state. The RST is used as a tool for reducing and choosing the most relevant sets of internal states for predicting the semen fertilization potential. Chosen optimal data set is input to constructed neural network with supervised learning algorithm for the prediction of semen quality. This paper demonstrates that the RST is an effective pre-processing tool for reducing the number of input vector to ANN without reducing the basic knowledge of the information system in order to increase prediction accuracy of the proposed system. The resulting system is a hybrid prediction system for medical database called an Intelligent Rough Neural Network System (IRNNS).**

Keywords: Artificial Neural Network, Machine learning technique, In-vitro fertilization, Rough sets theory (RST), Fertility rate prediction, IRNNS, Hybrid prediction system.

VII. INTRODUCTION

Several machine learning techniques or data mining tools like Artificial Neural Networks (ANN), Fuzzy logic and Rough Sets Theory (RST) are used for data classification. There have been number of research works and surging interests in ANN and developing hybrid system by combining other applications with ANN. The neural network and rough sets methodologies have their place among intelligent classification and decision support systems. Knowledge of the system can be seen as organized data sets with the ability to perform classification. Hence a formal framework capable of reasoning about classifications and delivering implicit facts from explicit knowledge would be helpful. The ANN and RST can be combined to obtain such a framework. This approach is based on the rough sets feature selection mechanism and neural networks efficient classification property. Traditional model construction and simulation data mining techniques perform poorly due to the highly non linear dynamics and overwhelming complexity of data being generated.

The knowledge acquired by ANN through training process is represented by the weights of the connections between the neurons, the threshold values and the activation function. Identifying the problem description at the neural level is not possible because of the implicit knowledge representation of the neuron; therefore, neural network often called as 'black boxes'. To improve the quality of the learning, the Rough Sets Theory (RST) is used to select key parameters before training the predictor (ANN).

Rough Sets Theory, developed by Z. Pawlak and his co-workers in the early 1980s [1], has become a widely recognized data analysis method to deal with vagueness and uncertainty of data [2]. The concept of RST is founded on the assumption that every object of the universe of discourse is associated with some information [3]. The RST finds the description of sets of objects in terms of attribute values, checks dependency between attributes, finds significance of attributes, reduces attributes and derives decision rules [4]. The rough sets based reduction of the attributes space not only improves the efficiency of the predictor itself, but also provides some additional information about the mechanisms governing decision-making. One of the reasons for developing hybrid system is to build more powerful systems that can reduce drawbacks of implementing a single machine learning techniques. Some of other researchers proposed similar integrated method in other applications for classification and prediction purpose [5]-[8].

In this paper, a quick reduct algorithm based on attribute frequency in discernibility matrix is proposed for pre-processing. We also propose an intelligent rough neural network algorithm for efficient data classification and prediction. The medical data used in this work are

in the format of multi-attribute information table and suit the rough set model. The paper is organized as follows. In Section II, the rough set and neural network approach is briefly reviewed. The hybrid strategy of proposed model in the data mining setting is presented. The RST based data analysis is reviewed in Section II-A, and ANNs are discussed in Section II-B. Then the overall structure of the hybrid system is presented in Section II-C. In Section III, illustrative experimental results are presented. Then this paper is concluded with brief discussion of the study and future research directions.

VIII. ROUGH SETS THEORY

The method of rough set data analysis has the following advantages over traditional methods [9], [10]. Rough set method is unlike probability in statistics or membership grade in the fuzzy set theory, based on the original data sets not any external information [11]. It is suitable for both quantitative, qualitative attributes and discovers hidden facts in data in the form of decision rules. The derived decision rules describe the knowledge contained in the information tables and eliminate the redundancy of original data. The results obtained by rough set method are simple and explainable. Finding minimal subsets (reducts) of attributes that are efficient for rule making is a central part of its process [12]. RST is a combinatorial tool for reducing quantized data sets by discarding attributes that have no or limited discriminatory power [2], [4] and [13].

A. Basic notions

The basic notions of RST are: *information system, approximations, reduction of attributes* and *others*.

1) Information system: An information system is defined as I=(U,A), where U is a non-empty set of finite objects called universe, the finite attribute set A=$\{a_1,.. a_n\}$, where each attribute $a \in A$ is a total function $a : U \rightarrow V_a$, where V_a is called the domain or value set of attribute a_i.

An approximation space is an ordered pair A = (U, R), where U is a finite and non-empty set of elements called attributes, R is an equivalence relation about U. Any set $B \subseteq A$ there is an associated equivalence relation called B-indiscerbility relation defined as:

$$IND_A(B) = \{(x, y) \in U^2 \mid \forall a \in B, a(x) = a(y)\} \quad \ldots \ldots (1)$$

If $(x, y) \in IND_A(B)$, then x and y are indiscernible from each other by attributes from B. The indiscernibility is an equivalence relation.

2) Approximations: In this way, RST provide a simple form to treat with the uncertainty. Given information system I, let $X \subseteq U$ be a set of objects and $B \subseteq A$ is a selected set of attributes. The lower and upper approximations of X with respect to B are defined as:

$$B_*(X) = \cup\{Y \in U \mid IND(P) : Y \subseteq X\}, \quad \ldots. \ldots. (2)$$

$$B^*(X) = \cup\{Y \in U \mid IND(P) : Y \cap X \neq \varphi\}. \ldots. \ldots. (3)$$

The *B*-lower approximation $B_*(X)$, is the complete set of objects in U which can be *certainly* classified as elements in X using the set of attributes B and the B-upper approximation $B^*(X)$, is the set of elements in U that can be *possibly* classified as elements in X. The B-boundary of X in the information system I, is defined as: $BND(X)= B^*(X) - B_*(X)$. The rough set approximations are illustrated in Fig. 1.

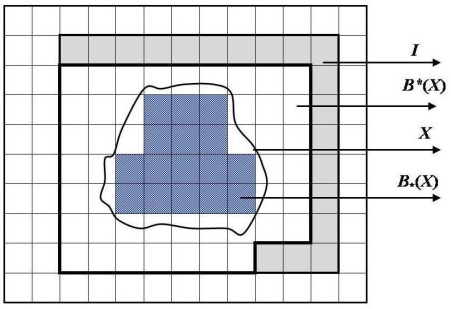

I – Information System,

B*(X)- Upper approximation,

Fig. 1. Rough set approximations

3) Reduction of Attributes: Reduct is a minimum attributes subset that retains the decision attributes dependence degree to conditional attributes. The subset $R \subseteq B \subseteq A$ such that $Y_B(Y)=Y_R(Y)$ is called Y-reduct of B and denoted as $Red_Y(B)$. The *core* is possessed by every legitimate *reduct* and cannot be removed from the information system without deteriorating basic knowledge of the system. The set of all indispensable attributes of B is called *Y*-core. Formally,

$$Core_Y(B) = \cap Red_Y(B) \quad \ldots \ldots \ldots \ldots (4)$$

The *Y-core* is intersection of all *Y-reducts* of *B*, included in every *Y-reducts* of *B*.

3) Accuracy: Accuracy measures how much a set is rough. If a set has $B_*(X) = B^*(X) = X$, the set is precise called *crisp* and for every element $x \in X \in U$. This is expressed by the formula:

$$\alpha_B(X) = \frac{|B_*(X)|}{|B^*(X)|} \quad \ldots\ldots\ldots\ldots\ldots (5)$$

When $0 \le \alpha_B(X) \le 1$, and if $\alpha_B(X) = 1$ X is crisp with respect to B.

IX. ARTIFICIAL NEURAL NETWORK

ANN is an interconnected group of artificial neurons that uses a mathematical model or computational model for information processing based on a connectionist approach to computation. In most cases an ANN is an adaptive system that changes its structure based on external or internal information that flows through the network. In more practical terms neural networks are non-linear statistical data modeling tools. They can be used to model complex relationships between inputs and outputs or to find patterns in data. As computers become faster, the ANN methodology is replacing many traditional tools in the field of knowledge discovery and some related fields. ANN is composed of a large number of highly interconnected processing elements (neurons) working in unison to solve specific problems. The learning in biological systems involves adjustments to the synaptic connections that exist between the neurons.

The main neural networks types based on their structures are Single layer perceptron, Multi-layer perceptron, Backpropagation net, Hopfield net and Kohonen feature map. Multi-layer perceptron (MLP) is recognized as the best ANN used in classification from examples [14]. In this work, the *multi-layer perceptron* with *back-propagation* supervised learning algorithm is used for experimentation. Due to its extended structure, MLP is able to solve every logical operation, including XOR problem. The back-propagation algorithm in MLP is the solution of choice for many machine learning tasks [15],[16]. An advantage of supervised learning is the minimization of error between the desired and computed unit values. The predictive performance of ANN is measured by computing the mean squared error (MSE), defined as:

$$MSE = \frac{1}{NP} \sum_{j=0}^{P} \sum_{i=0}^{N} (d_{ij} - y_{ij})^2 \quad \ldots\ldots (6)$$

where P is number of output processing elements, N is number of exemplars in the data set, y_{ij} is network output for exemplar i at processing element j and d_{ij} is target output for exemplar i at processing element j.

IV. INTELLIGENT ROUGH NEURAL NETWORK SYSTEM (IRNNS)

1) The framework of hybridizing RST and ANN-based Set all weights of units to random values ranging from -1.0 to +1.0.
2) Set an input pattern to the neurons of the net's input layer.
3) Activate each neuron of the following layer.

learning system is shown in Fig. 2 and 3. These two techniques can be used for both classification and regression tasks without any converting mechanism. Incorporating these two technologies in one as an Intelligent Rough Neural Network System for efficient processing of medical data base is described in this section. The proposed hybrid system uses RST for pre-processing of data and ANN for classification or prediction. Some researchers have proposed and used similar integrated method in other applications [5], [6]. An algorithm developed for proposed hybrid system is given below and illustrated in Fig. 2.

A. Algorithm for Intelligent Rough Neural Network System

Algorithm: IRNNS

Given: Medical data set.

Objective: Obtain crisp set of influential parameters and construct suitable ANN architecture for prediction.

// Pre-processing phase using RST.//

Step 1. Discretize the data.

Step 2. Construct the information system.

Step 3. Select influential parameters in the form of reduct set by applying Reduct algorithm.

Step 4. Check the selected parameters by considering biological importance. If satisfied go to Step 5 for training ANN *else* go to Step 1.

// ANN construction and training phase.//

Step 5. Data set (i_n, t_n) n = 1,2, … k, where input i_n and target t_n. Split the data into three subsets as training, cross-validation and test sets.

Step 6. Construct suitable ANN architecture. Structuring ANN with supervised back propagation learning algorithm includes following steps:

1) Set all weights of units to random values ranging from -1.0 to +1.0.
2) Set an input pattern to the neurons of the net's input layer.
3) Activate each neuron of the following layer.

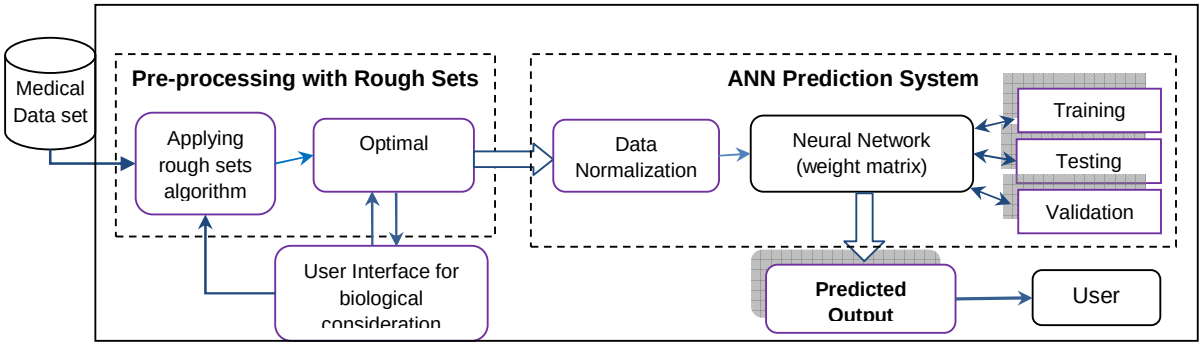

Fig. 2. Overview of Hybrid IRNNS Model

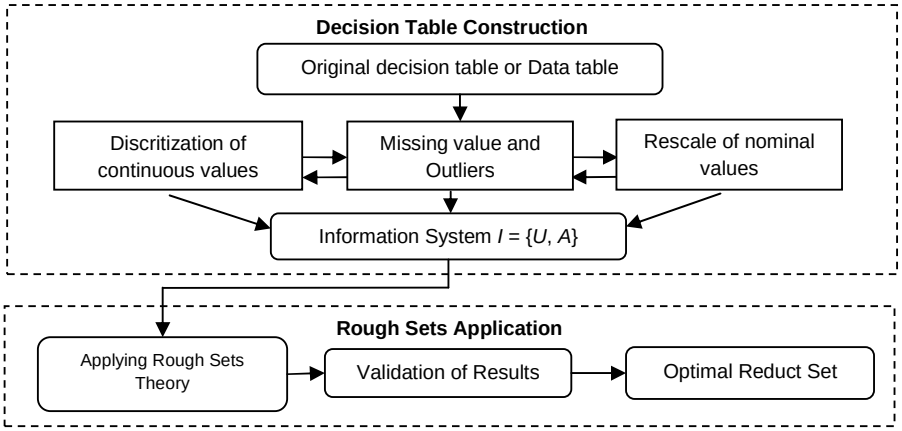

Fig. 3. Different stages of Pre-processing with Rough Sets

(Multiply the weight values of the connections leading to the neuron with the output values of the proceeding neurons and add up these values. Pass the result to an activation function, which computing the output value of this neuron.)

4) Repeat this until the output layer is reached.
5) Compare the calculated output pattern to the desired target pattern and compute an error value.
6) Change all weights of each weight matrix using the formula
*Weight (old) + learning rate * output error * output (neurons i) * output (neurons i+1) * (1 - output (neurons i+1))*

7) Go to Step 2.

8) The algorithm ends, if all output patterns match their target patterns.

Step 7. Now, the constructed ANN is ready for prediction or classification.

(The performance of this network was subsequently optimized by varying the number of nodes in the hidden layer and remove redundant nodes.)

B. Pre-processing with Rough sets theory

The rough sets based reduction of attribute space improves the efficiency of the predictor itself [13], [17]. The RST pre-processing model consists of two stage approaches, the first stage involves decision table reconstruction and the second stage involves the application of optimal reduct algorithm for data analysis. The different stages of data analysis using rough sets model is illustrated in Fig. 3. The algorithm used in IRNNS is described below.

1) Quick Reduct Algorithm: The basic concept is that intersection of every items of discernibility matrix and reduct cannot be empty. The object of matrix i and j would be indiscernible to the reduct, if there are any empty intersections between items c_{ij} with reduct, this contradicts the definition that reduct is the minimal attribute set discerning all objects.

Let reduct set *OptRed* =ϕ. Sort the discernibility matrix $|c_{ij}|$ and examine every items of discernibility matrix c_{ij}. If their intersection is empty, a shorter and frequent attribute $|c_{ij}|$ is picked and inserted in *OptRed* and skip the entry otherwise. Attributes in shorter and frequent contribute more classification power to the reduct. If there is only one element in c_{ij}, it must be a member of reduct. Repeat the procedure until all entries of discernibility matrix are examined. Finally, we get the optimal reduct in *OptRed*.

Algorithm: Quick reduct algorithm
Input: an information system (U, $A \cup \{d\}$),
where $A = \cup a_i$, $i = 1,\ldots,n$.
Output: an optimal attribute set *OptRed.*
Step 1. $OptRed = \phi$, $freq(a_i) = 0$, for $i = 1,\ldots n$.
Step 2. Generate discernibility matrix *DisMat.*
Step 3. Count frequency of every attribute a_i in *DisMat;*
$freq(a_i) = freq(a_i) + n / |c|$ *for every* $a_i \in |c|$
Step 4. Merge and sort discernibility matrix *DisMat.*
Step 5. For every object c_{ij} in *DisMat* Do
{
Step 6. if ($c_{ij} \cap OptRed == \phi$) then
{
Step 7. Select attribute a_i with maximal $freq(a_i)$ in *OptRed.*
Step 8. $OptRed = OptRed \cup \{a\}$.
}
}
Step 9. Return *OptRed*

The quick reduct algorithm can be very useful for classifying unseen objects [18]. The idea of the algorithm is, taking frequency of attribute as heuristic. The technique is also applicable to optimal/approximate rule generation for they are also based on discernibility matrix. The middle- sized noisy dataset can be reduct by this algorithm, and can be used as input for ANN for further optimal classification / prediction.

V. ILLUSTRATIVE EXPERIMENTS

To illustrate the use of proposed hybrid method of data classification, let us consider an example of spermatalogical data set from the in-vitro fertilization (IVF) test outcomes for predicting bulls' semen fertility rate. The outcomes of the experiments are consulted with experts while selecting significant parameters using RST.

A. Data Set

The spermatological data used in the experiments are collected from Reproductive physiology laboratory in National Institute of Animal Nutriton and Physiology, Bangalore. The sperm functional parameters such as progressive forward motility, plasmalemma integrity, acrosomal integrity, sperm nuclear morphology and mitochondrial membrane potential were collected. The

percentage of observed cleavage rate was calculated by dividing the number of oocytes cleaved out of the total number of oocytes inseminated.

B. Application of rough sets theory in semen evaluation

Rough set theory is used for finding most effective minimal sperm functional attributes known as *reduct* set; those are effective in predicting cleavage rate or fertilization potential. When evaluating semen, the ultimate goal is to accurately predict its fertilizing potential [19].

The decision table, representing the spermatological data set, is constructed using eight condition attributes and one decision attribute of observed cleavage rate. In order to get better results, the data set is normalized by selecting maximum value and dividing all other values by the maximum value, the method generally used for normalizing input to neural network [20]. Since the new decision table contains discrete set of values, it does not require further discretization when considering indiscernibility relation. The next step is creating reducts, which are subset vectors of attributes that facilitate rule generation with minimal subsets. The proposed quick reduct algorithm is applied for creating minimal attribute set called *reduct*. The idea of the algorithm is taking frequency of attribute as heuristic, and it is worth to mention that applying reduction algorithm to get minimal subset of attributes is an NP-hard problem [21]. To calculate frequency of attributes, discernibility matrix is constructed and sorted. Every items of discernibility matrix C_{ij} is examined and shorter and more frequent attribute $\{a_6\}$ is picked and assigned in *OptRed*. As known, attributes in shorter and frequent contribute more classification power to the reduct. The attribute $\{a_6\}$ is only one element, so it is a member of reduct as per algorithm. By repeating the procedure until all entries of discernibility matrix are examined, we get optimal reduct in *OptRed* (e.g. Table 2). The obtained optimal reduct set contains all the classification power of original decision table. All other possible reduct sets based on indiscernibility matrix are shown in Table 1.

TABLE 1
POSSIBLE REDUCT SETS BASED ON INDISCERNIBILITY MATRIX

Reduct Sets	Support	Length
$\{a_3,a_4,a_6\}$	100	3
$\{a_1,a_3,a_8\}$	100	3
$\{a_1,a_3,a_4\}$	100	3
$\{a_3,a_6,a_8\}$	100	3
$\{a_4,a_6,a_8\}$	100	3
$\{a_1,a_4,a_8\}$	100	3

The biological importances of the parameters are considered while obtained optimal reduct set. If obtained reduct sets are not satisfied considering their biological importance, control goes to step 1 of the IRNNS algorithm. The reduced / crisp data set is effective to train ANN. The experiments to determine the prediction accuracy of ANN is described in the remaining part of this section.

TABLE 2
OPTIMAL REDUCT SET OBTAINED BY APPLYING QUICK REDUCT ALGORITHM AND CONSIDERING BIOLOGICAL IMPORTANCE

Optimal Reduct Set	Support	Length
$\{a_1,a_3,a_4,a_6,a_8\}$	100	5

C. Network training and classification

The constructed sample multi-layer perceptron (MLP) structured ANN is used for the prediction of animal semen fertility rate using obtained influential IVF parameters. The multi-layer perceptron (MLP), used to devise model of ANN, is illustrated in Fig. 4.

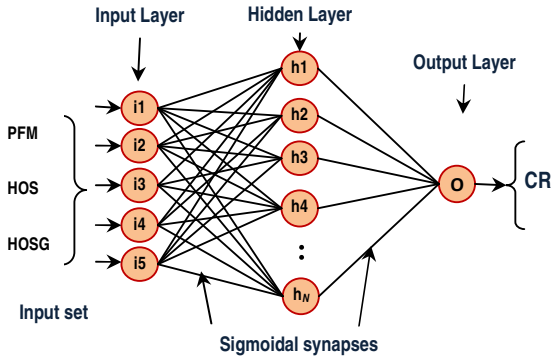

PFM – Progressive forward motility, HOS - Hyposomotic swelling test, SNM – Sperm nuclear morphology, MMP – Mitochondrial membrane potential, SZB – Sperm-zona binding, CR – Predicted Cleavage rate

Fig. 4. The constructed sample multi-layer perceptron (MLP) for predicting semen fertility rate.

Different processes involved in the optimization of ANN are: (1) selecting training and validation subsets, (2) analysing and transforming data, (3) selecting variables, (4) network construction and training, and (5) model verification. A properly trained ANN is capable of generalizing the information on the basis of the

knowledge acquired during the training phase and correctly infers the unseen part of population even if the sample data contain noisy information. To train ANN, a suitable training, validation and test sets are selected. In this work, the training, validation, and test sets are provided by the following parameters.

- PFM - Progressive forward motility
- HOS – Hypoosmotic swelling test
- HOSG – Hypoosmotic swelling and Giemsa test
- SNM – Sperm nuclear morphology
- SZB – Sperm zonapellula bining

The target set is composed by the (CR) observed cleavage rate. The target set corresponding to the training set is directly provided by recorded field fertility rate of animals. The input set values are pre-processed in order to guarantee that all training values will be converted into the range of possible outputs of the network, and so the network can be trained. Descriptive statistics for all quantitative input variables to train ANN is illustrated in Table 3.

TABLE 3
DESCRIPTIVE STATISTICS FOR ALL QUANTITATIVE INPUT VARIABLES TO TRAIN ANN

Selected Parameters	Mean ± S.E.	Minimum	Maximum
PFM	43.25 ± 2.69	36.27	49.31
HOS	39.58 ± 2.32	31.85	47.68
HOS-G	30.63 ± 4.56	24.71	39.39
SNM	70.14 ± 7.5	65.02	74.66
SZB	88.27 ± 3.18	73.77	107.09
CR	38.07	8.63	48.01

The computer simulations of biological neuron layers of ANN are created. The MLP shown in Fig. 4., has the following characteristics:

1. *input layer:* 5 nodes as selected parameters for training are five;
2. *hidden layer:* one hidden layer with 10 nodes (fixed after analysis);

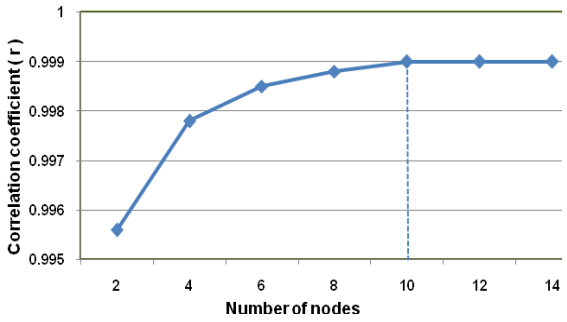

Fig. 5. Optimum number of nodes for the hidden layer

3. *output layer:* output layer has one node as constructed neural network would be used to predict a fertility rate

The performance of this network was subsequently optimized by varying the number of nodes in the hidden layer, the learning coefficient and the decrease factor of this coefficient and selecting the configuration with the highest predictive ability is illustrated in Fig. 5. Once trained, the network is ready to run validation and test set. The ANN validation phase in our experiment is shown in Fig. 6. Now, the ANN is trained well and ready for the prediction phase.

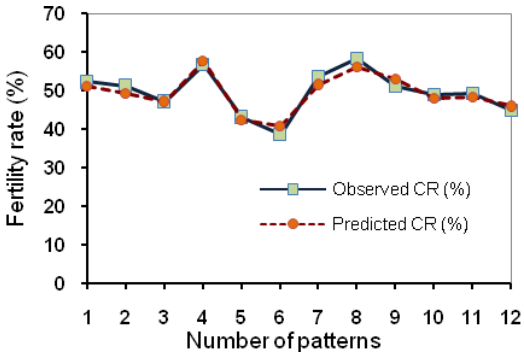

Fig. 6. Desired and actual output of ANN during validation test.

D. Results

The proposed hybrid prediction system is applied for pre-processing of medical database and to train ANN for making prediction. The prediction accuracy is observed by comparing observed and predicted cleavage rate (e.g. Fig. 7.).

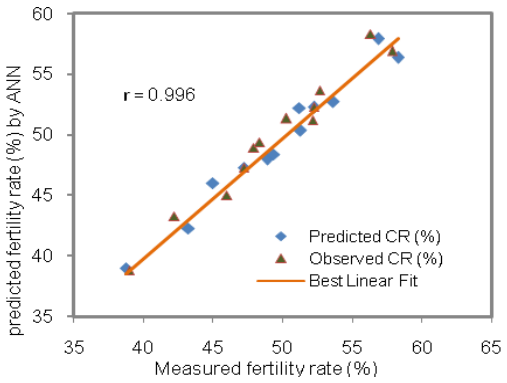

Fig. 7. Prediction accuracy: comparison between observed and predicted cleavage rate.

VI. CONCLUSIONS AND FUTURE WORK

The experimental results show that the proposed hybrid architecture is very efficient for medical data analysis in significantly lesser processing time. Since RST is a useful tool for incomplete or noisy data processing, proposed hybrid architecture is a promising and intuitively sound methodology for large or medium size medical data base with incomplete data.

In addition, the results show that the hybridization of two machine learning techniques like ANN and RST is a promising alternative to the conventional methods of data analysis in this era of fast computers. The training time of the ANN with reduced sets of inputs is also quite naturally shorter and improves prediction accuracy.

The RST is useful pre-processing tool for the input to ANN to improve classification and prediction. It is observed from the experiments that the hybridization of RST and ANN significantly improves the overall predictive ability of ANN. The proposed hybrid method is quite effective for classifying pattern from abundant and noisy data. The hybrid strategy is accepted as a valid approach to data mining, because no single method has enough capability to deal with various data mining settings.

Future work involves incorporating biological information into the model. Another direction for the future work involves systematic comparison of different machine learning algorithms, hybridization of rough sets and neural network ensembles for building predictors to improve performance more.

Z. Pawlak, "Rough sets," International Journal of Computer and Information Sciences, pp. 11:341-346, 1982.
Z. Pawlak, "Rough Sets: Theoretical Aspects of Reasoning About Data," Kluwer Academic Publishers, Boston, MA, 1991.
E.H. Francis Tay and Lixiang Shen, "Economic and financial prediction using rough sets model, Computing, Artificial Intelligence and Information Technology," European Journal of Operational Research, vol. 141, pp. 641-659, 2002.
Z. Pawlak, "Rough sets," Rough Sets and Data Mining," Kluwer Academic Publisher, Dordrecht, pp. 3-8, 1997.
Yu Wang, Mingyue Ding, Chengping Zhou and Tianxu Zhang, "A Hybrid Method for Relevance Feedback in Image Retrieval Using Rough Sets and Neural Networks", International Journal of Computational Cognition, vol. 3:1, 2005.
B.S. Ahn, S.S. Cho, and C.Y. Kim, "The integrated methodology of rough set theory and artificial neural network for business failure prediction," Expert Systems with Applications, vol. 18, pp. 65-74, 2000.
M. Beri, and G. Trotta, "An Approach to Develop Classification Expert Systems with Neural Network," Computational Intelligence III, Elsevier science, Netherlands, 1991.
Y. Hayashi, "A Neural Expert System Using Fuzzy Teaching Input", In Proceedings of 92 IEEE International Conference on Fuzzy System FUZZ-IEEE, Piscataway, NJ, pp. 485-491, 1992.
A.I. Dimitras, R. Slowinski, R. Susmaga, and C. Zopounidis, "Business failure prediction using rough sets," European Journal of Operational Research, vol. 114, pp. 263-280, 1999.
S. Greco,B. Matarazzo, and R. Slowinski, "A new rough set approach to evaluation of bankruptcy risk," Operational Tools in the Management of Financial Risks, Kluwer Academic Publishers, Dordrecht, pp. 121-136, 1998.
E. Krusinska, R. Slowinski, and J. Stefanowski, "Discriminant versus rough set approach to vague data analysis," Applied Stochastic Models and Data Analysis, vol. 8, pp. 43-56, 1992.
J. Han and M. Kamber, "Data mining: concepts and techniques," Morgan Kaufmann Publishers, San Francisco, 2001.
Tomasz G. Smolinski, Darrel L. Chenoweth, and Jacek M. Zurada, "Application of Rough Sets and Neural Networks to Forecasting University Facility and Administrative Cost Recovery," Artificial Intelligence and Soft Computing, vol. 3070, 2004.
Yaile Caballero, Rafael Bello, Yanitza Salgado and Maria M. Garcia, "A Method to Edit Training Set Based on Rough Sets," International Journal of Computational Intelligence Research, vol. 3:3, pp. 219-229, 2007.
M. Durairaj and K. Meena. "Application of Artificial Neural Network for Predicting Fertilization Potential of Frozen Spermatozoa of Cattle and Buffalo," International Journal of Computer Science and System Analysis, pp. 1-10, 2008.
B. Yegnanarayana, "Artificial Neural Network," Eastern Economy Edition, 2001.
M. Durairaj and K. Meena, "Intelligent Classification Using Rough Sets and Neural Networks," The ICFAI Journal of Information Technology, vol. 3, pp.75-85, 2007.
K. Thangavel, P. Jaganathan, A. Pethalakshmi and M. Karnan, "Effective Classification with Improved Quick Reduct For Medical Database Using Rough System," BIME Journal, vol. 5:1, 2005.
Leonardo F.C. Brito, Albert D. Barth, "Comparison of methods to evaluate the plasmalemma of bovine sperm and their relationship with in vitro fertilization rate," Theriogenology, Elsevier, pp. 1539-1551, 2003.
A. Chouchoulas, J. Halliwell, and Q. Shen, "On the Implementation of Roush Set Attribute Reduction," In Proceedings of the 2002 UK Workshop on Computational Intelligence, pp. 18-23, 2002.
W. Ziroko, "The Discovery, Analysis, and Representation of Data Dependencies in Databases," in G. Piatctsky-Shapiro, and W. Frawley, (cds), Knowledge Discovery in Databases, AAAI/ MIT Press, Cambridge, MA, pp. 31-54, 1990.

INTERNATIONAL JOURNAL OF INNOVATIVE TECHNOLOGY & CREATIVE ENGINEERING (ISSN:2045-8711)
VOL.1 NO.7 JULY 2011

Flow Of Herschel – Bulkley Fluid In An Inclined Flexible Channel Lined With Porous Material Under Peristalsis

S.Sreenadh [1], S.Rajender [1], S.V.H.N.Krishna Kumari.P[2],Y.V.K.Ravi Kumar[3]

[1] *Department of Mathematics, Sri Venkateswara University, Tirupati, INDIA.*
[2] *Department of Mathematics, Bhoj Reddy Engineering College for women, Hyderabad, INDIA.*
[3] *Department of Mathematics, Stanley College of Engineering and Technology women, Hyderabad, INDIA.*
(Corresponding author, yvkravi@rediffmail.com)

***Abstract*— This paper is concerned with the study of the peristaltic flow of Herschel – Bulkley fluid in an inclined flexible channel lined with porous material under long wave length and low Reynolds number assumptions. This model may be applicable to describe blood flow in the sense that erythrocytes region and the plasma regions may be described as plug flow and non-plug flow regions. The effect of yield stress , Darcy number ,angle of inclination and the index on the flow characteristics is discussed through graphs.**

Keywords: peristaltic flow,Herschel – Bulkley fluid, inclined channel.

X. INTRODUCTION

Peristaltic transport is a form of fluid transport which occurs in biological systems. This mechanism has received considerable attention in recent times in engineering as well as in medicine. It plays an indispensable role in transporting many physiological fluids in the body. Many modern mechanical devices have been designed on the principle of peristaltic pumping for transporting noxious fluids without contaminating the internal parts. Further the blood transfusion process in dialysis, the mechanism of peristalsis may be applicable since the blood flow in small blood vessels is reported to be done by peristalsis.

Latham (1966) made first experimental study of the mechanics of peristaltic transport. The results of the experiments were found to be in good agreement with the theoretical results of Shapiro (1967). Based on this experimental work, Burns and Parkes (1967) studied the peristaltic motion of a viscous fluid through a pipe and a channel by considering sinusoidal variations at the walls.

In physiological peristalsis, the pumping fluid may be a Newtonian or non – Newtonian fluid. Kapur (1985) suggested several mathematical models for pumping physiological fluids. Among these some models deal with Newtonian fluids and others with non – Newtonian fluids. Ravi Kumar et al. [ ] studied the peristaltic pumping in a finite length tube with permeable wall. Krishna Kumari et al. [ ] studied the peristaltic pumping of by considering Jeffrey model.

Scott Blair (1959) reported that blood obeys the Casson model only for moderate shear rate flows. He also reported that the assumptions included in Casson's equation are not suitable for Cow's blood and that the Herschel – Bulkley equation represents fairly closely what is occurring in the blood. Herschel – Bulkley fluid is a semi solid rather than an actual fluid.

Among models of semisolids, the Herschel – Bulkley model is preferred because it describes blood behaviour very closely and also the Newtonian, Bingham and Power – law models can be derived as special cases. Furthermore, Herschel – Bulkley fluids describe flows with a non –linear stress strain relationship either as a shear thickening fluids or shear thinning one. Since shear thinning and shear thickening fluids play an important role in biomedical engineering.

Some examples of fluids behaving in this manner include food products, pharmaceutical products, slurries, polymeric solutions and semisolid materials. Chaturani and Samy (1985) discussed the blood flow through a stenosed artery by considering blood as a Herschel – Bulkley fluid. The gastrointestinal tract is surrounded by a number of heavily innervated smooth muscle layers, contraction of these muscle layers can mix the contents of the tract and move food in a controlled manner in an appropriate direction. Epithelial cells, beneath these layers are responsible for the absorption of nutrients and water from the intestine. These layers consist of many folds and there are pores through the tight junctions of them. So the flow of fluids in different geometries in channels/tubes with porous material at the boundary is very significant in physiological applications. Vajravelu et al.[ ] considered the Herschel – Bulkley fluid in their study of peristaltic pumping of fluids.

In view of these, peristaltic flow of Herschel – Bulkley fluid in an inclined flexible channel lined with porous material is studied under long wave length and low Reynolds number assumptions. This model may be applicable to describe blood flow in the sense that erythrocytes region and the plasma regions may be described as plug flow and non-plug flow regions.

HERSCHEL – BULKLEY MODEL

The basic equations governing the flow of an incompressible Navier-Stokes fluid are the field equations

div V = 0,

$$div\sigma + \rho f = \frac{dv}{d\tau}$$

where V is the velocity, f the body force per unit mass, ñ the density, and d*/*dt the material time derivative. ó is the Cauchy stress defined by

$$\sigma = -pI - T$$

$$T = 2\mu D + S, \quad S = 2\eta D$$

where **D** is the symmetric part of the velocity gradient, that is,

$$D = \frac{1}{2}\left[L + L^T\right], L = grad\, V$$

Also $-\rho l$ denotes the indeterminate parof the stress due to the constraint of incompressibility, μ and **c** are viscosities.

The Herscel-Bulkely model combines the effects of Bingham and power-law behaviour in a fluid. For low strain rates $\left(\gamma < \tau_0 / \mu_0\right)$, the "rigid" material acts like a very viscous fluid with viscosity μ_0. As the strain rate increases and the yield stress threshold, τ_0 is passed, the fluid behaviour is described by a power law

$$\eta = \frac{\tau_0 + k[\dot{\gamma}^n - (\tau_0 / \mu_0)^n]}{\dot{\gamma}}$$

where k is the consistency factor and n is the power-law index.

II. MATHEMATICAL FORMULATION

Consider the peristaltic pumping of a Herschel – Bulkley fluid in an inclined flexible channel of width 'a'. The channel is inclined at an angle θ with the horizontal. The flexible walls of the channel are coated with non erodible porous material. Suppose we have a longitudinal train of progressive sinusoidal waves on the upper and lower walls of the channel. For simplicity, we restrict our discussion to the half width of the channel as shown in Fig. 1. The region between y=0 and y = y_0 is called a plug flow region. In the plug flow region, $|\tau_{xy}| \le \tau_0$. In the region between y = y_0 and y = H, we have $|\tau_{xy}| \ge \tau_0$.

The wall deformation is given by

$$Y = H(X, t) = a + b \sin\frac{2\pi}{\lambda}(X - ct) \qquad (1)$$

where b is the amplitude , λ is the wavelength and c is the wave speed.

Under the assumptions that the channel length is an integral multiple of the wavelength λ and the pressure difference across the ends of the channel is a constant, the flow becomes steady in the wave frame (x,y) moving with the velocity c away from the fixed (laboratory) frame (X,Y) .

The transformation between these two frames is given by

x = X-ct , y = Y , u(x,y) = U (X-ct, Y) – c

v(x,y) = V(X-ct , Y) , p(x) = p(X,t) , ⊖ = ❤-Y (2)

where U and V are velocity components in the laboratory frame and u, v are velocity components in the wave frame and ⊖ and ❤ are the stream functions in the wave and laboratory frames respectively. In many physiological situations it is proved experimentally that the Reynolds number of the flow is very small. We assume that the flow is inertia free and the wavelength is infinite.

We introduce the following non-dimensional quantities in order to make the basic equations and boundary conditions dimensionless.

$$\bar{x}=\frac{x}{\lambda};\quad \bar{y}=\frac{y}{a};\quad \bar{h}=\frac{h}{a};\quad \bar{t}=\frac{ct}{\lambda};\quad \bar{\varepsilon}=\frac{\varepsilon}{a};$$

$$\phi=\frac{b}{a};\quad \bar{\tau}_0=\frac{\tau_0}{\mu\left(\frac{c}{a}\right)^n};\quad \bar{\psi}=\frac{\psi}{ac};\quad \bar{q}=\frac{q}{ac};\ \bar{F}=\frac{fa}{\mu\lambda c};$$

$$\bar{u}=\frac{u}{c}=\frac{\partial\psi^{(1)}}{\partial\psi y_0}\quad \bar{v}=\frac{v\lambda}{ac}=-\frac{\partial\psi}{\partial x};\ \bar{p}=\frac{pa^2}{\mu\lambda c};$$

where $\bar{\mu}$ and $\bar{\upsilon}$ are velocity components in the wave frame.

Under the lubrication approach, the equations governing the motion become (dropping bars)

$$\frac{\partial}{\partial y}\left(\tau_{yx}\right)=-\frac{\partial p}{\partial x}+\eta\sin\theta \qquad (3)$$

where $\tau_{yx}=\left(-\frac{\partial u}{\partial y}\right)^n+\tau_0$ (4)

The dimensionless boundary conditions are

$\psi=0$ at $y=0$ (2) (5)

$\psi_{yy}=0$ at $y=0$ (6)

$\tau_{yx}=0$ at y = 0 (7)

$u=\frac{-\sqrt{Da}}{\alpha}\frac{\partial u}{\partial y}-1$ at $y=h(x)-\varepsilon$ (8)

III. SOLUTION OF THE PROBLEM

On solving equations (3) and (4) together with boundary conditions (5) - (8) and $u=\frac{\partial\psi}{\partial y}$ and $\upsilon=-\frac{\partial\psi}{\partial x}$, we get the velocity field as

$$u=P^k\left[\frac{1}{K+1}\left\{\left(h-\in-y_0\right)^{k+1}-\left(y-y_0\right)^{k+1}\right\}+\frac{\sqrt{Da}}{\alpha}\left(y-y_0\right)^k\right]-1 \qquad (9)$$

where $p=-\frac{\partial p}{\partial x}+\eta\sin\theta:\ k=\frac{1}{n}$ (10)

We find the upper limit of the plug flow region using the boundary conditions that $\psi_{yy}=0$ at $y=y_0$ so, we have, $y_0=\frac{\tau_0}{P}$ (11)

Also by using by the condition

$\tau_{yx} = \tau_{h-\in}$ at $y = h-\in$, we obtain

$$P = \frac{\tau_{h-\in}}{h-\in} \qquad (12)$$

Hence $\frac{y_0}{h-\in} = \frac{\tau_0}{\tau_{h-\in}} = \tau; 0 < \tau < 1$

Taking $y = y_0$ in (9) we get the velocity in the plug flow region as

$$u_p = \frac{p^K}{k+1}\left[h-\in -y_0\right]^{k+1} - 1 \qquad (13)$$

Integrating equations (9) and (13) and using the conditions $\psi_p = 0$ and $\psi = \psi_p$ at $y = y_0$ we get the stream function as

$$\psi = -y + p^k\left\{\frac{1}{k+1}[h-\varepsilon-y_0]^{k+1}y - \frac{(y-y_0)^{k+2}}{k+2}\right\} + \frac{\sqrt{Da}}{\alpha}\frac{(y-y_0)^{k+1}}{k+1} \qquad (14)$$

$$\psi_p = -y + \frac{p^k}{k+1}\left[\left(h-\in -y_0\right)\right]^{k+1} y \qquad (15)$$

The volume flux 'q' through each cross section in the wave frame is given by

$$q = \int_0^{y_0} u_p dy + \int_{y_0}^{h-t} u dy$$

$$= -(h-\varepsilon) + \frac{p^k}{k+1}[(h-\varepsilon-y_0]^{k+1}(h-\varepsilon) - (h-\varepsilon-y_0)^{k+1}\left(\frac{h-\varepsilon-y_0}{k+2} + \frac{\sqrt{Da}}{\alpha}\right) \qquad (16)$$

The Instantaneous volume flow rate $Q(X,t)$ in the laboratory frame between the central line and the wall is

$$Q(X,t) = \int_0^H U(X,Y,t)\,dY \qquad (17)$$

From equation (16) we can write

$$\frac{dp}{dx} = -\left\{\frac{(q+h-\in)(k+1)(k+2)\alpha}{\left[(h-\in)^{k+2}(1-\tau)^{k+1}(k+2)\alpha\right] - (h-\in)^{k+1}(1-\tau)^{k+1}\left[(h-\in)(1-\tau) + \sqrt{Da}(k+2)\right]}\right\}^{\frac{1}{k}} + \eta\sin\theta \qquad (18)$$

Averaging equation (17) over one period yields the time mean flow (time - averaged volume flow rate) $\bar{Q}$ as

$$\bar{Q} = \frac{1}{T}\int_0^T Q\,dt = q+1 \qquad (19)$$

The pumping characteristics

Integrating the equation (18) with respect to 'x' over one wavelength, we get the pressure rise (drop) over one cycle of the wave as

$$\Delta P = -\int_0^1 \left[\left\{ \frac{(Q-1+h-\epsilon)(k+1)(k+2)\alpha}{\left[(h-\epsilon)^{k+2}(1-\tau)^{k+1}(k+2)\alpha\right]-(h-\epsilon)^{k+1}(1-\tau)^{k+1}\left[(h-\epsilon)(1-\tau)+\sqrt{Da}\,(k+2)\right]} \right\}^{\frac{1}{k}} + \eta\sin\theta \right] dx \tag{20}$$

The time averaged flux at zero pressure rise is denoted by $\bar{Q}_0$ and the pressure rise required to produce zero average flow rate is denoted by ΔP_0.

$$\Delta P = -\int_0^1 \left[\left\{ \frac{(-1+h-\epsilon)(k+1)(k+2)\alpha}{\left[(h-\epsilon)^{k+2}(1-\tau)^{k+1}(k+2)\alpha\right]-(h-\epsilon)^{k+1}(1-\tau)^{k+1}\left[(h-\epsilon)(1-\tau)+\sqrt{Da}\,(k+2)\right]} \right\}^{\frac{1}{k}} + \eta\sin\theta \right] dx \tag{21}$$

The dimensionless frictional force F at the wall across one wavelength is given by

$$F = \int_0^1 h\left(-\frac{dp}{dx}\right) dx$$

$$F = -\int_0^1 \left[\left\{ \frac{h(-1+h-\epsilon)(k+1)(k+2)\alpha}{\left[(h-\epsilon)^{k+2}(1-\tau)^{k+1}(k+2)\alpha\right]-(h-\epsilon)^{k+1}(1-\tau)^{k+1}\left[(h-\epsilon)(1-\tau)+\sqrt{Da}\,(k+2)\right]} \right\}^{\frac{1}{k}} + \eta\sin\theta \right] dx \tag{22}$$

IV. DISCUSSION OF RESULTS

The variation of pressure rise with time averaged flux is calculated from equation (20) and is shown in Fig. (2) for different values of yield stress with $\eta = 3$, $Da = 0.01, \alpha = 0.01, \theta = 0, \phi = 0.6, \epsilon = 0.1$ and $\eta = 0.2$. The pumping curves intersect at a point (0.5, 0.006) in the first quadrant due to variation in the parameter τ. It is found that ΔP increases with the increase in yield stress τ to the left of the point of intersection and opposite behaviour is observed to the right of this point. For a fixed ΔP, the flux increases due to an increase in the yield stress parameter τ in the first half of the channel.

The variation of ΔP with $\bar{Q}$ for different values of τ for $\theta = \pi/3$ is shown in Fig. (3). We find that the behaviour is same for horizontal and inclined channels.

The variation of pressure rise with time averaged flex is numerically evaluated for different values of Darcy number 'Da' with $n = 3, \alpha = 0.01, \phi = 0.6, z = 0.1$ and is shown in Fig. (4).It is observed that for a given Δp, the flux decreases with an increase in the Darcy number for $0 < \bar{Q} < 0.5$ and the opposite behaviour is observed for $0 < \bar{Q} < 0.5$. For a given flux $\bar{Q} > 0.5$, the pressure difference ΔP decreases with an increase in Da and the behaviour is found to be opposite for $\bar{Q} > 0.5$.

The variation of pressure rise Δp with the flux $\bar{Q}$ is calculated for different values of '$\in$' with $\theta = \pi / 3$, $\phi = 0.6$, $\tau = 0.1$ and $\alpha = 0.01$ and is shown in Fig. (5.) It is found that for a given '$\in$' (thickness of the porous lining), Δp decreases with the increase in the time averaged flux $\bar{Q}$. For a given $\bar{Q}$ >0.5 (approximately), Δp increases with the increasing $\in$ and $\bar{Q} > 0.5$ the variation of Δp is negligible.

The variation of pressure rise with $\bar{Q}$ for different values of angle of inclination 'θ' for different values of angel of inclination 'θ' is shown in Fig (6). It is observed that for a given Δp, the flux $\bar{Q}$ increases with the angle of inclination of the channel with the horizontal. For a given $\bar{Q}$, it is found that the pressure rise increases with the thickness of the porous lining.

The variation of pressure rise with time averaged flux is calculated for different values of n (index) and is shown in Fig.(7). We observe that the pumping curves intersect at a point (0.5, 0.17) in the first Quadrant. For a given Δp, we find that the flux $\bar{Q}$ decreases with an increase in index, 'n' for $0 < \bar{Q} < 0.5$ hen $\bar{Q} > 0.5$, the opposite behaviour is noticed. For a given flux $\bar{Q} < 0.5$. The pressure rise decreases with increasing 'n'. The opposite behaviour is observed for $\bar{Q} > 0.5$.

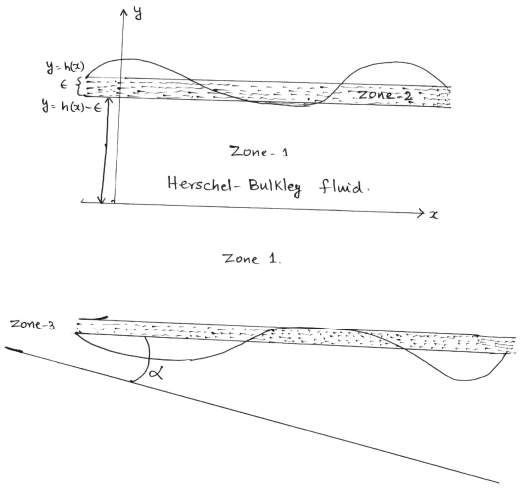

Fig.1. Physical model

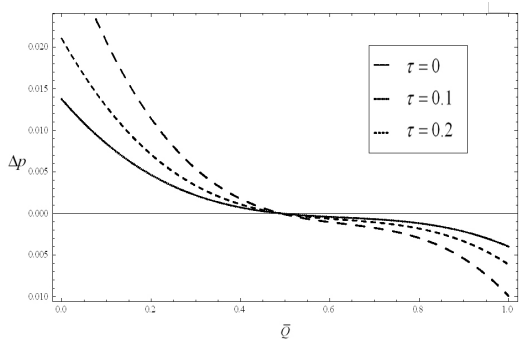

Fig 2. Variation of Δp with $\bar{Q}$ for different values of τ when n = 3,Da = 0.01, $\alpha = 0.01,\ \theta = 0,\ \in = 0.1,\ \phi = 0.6,\ \eta = 0.2$

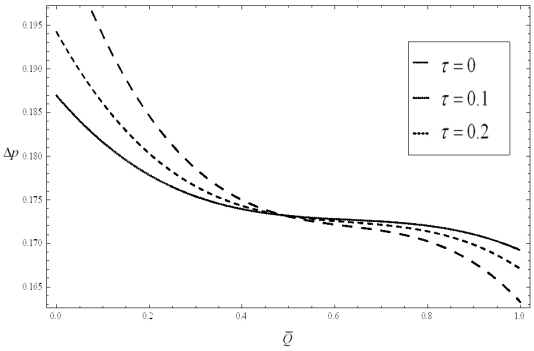

Fig 3. Variation of Δp with $\bar{Q}$ for different values of τ when n = 3,Da = 0.01, $\alpha = 0.01,\ \theta = \pi/3, \in = 0.1, \phi = 0.6, \eta = 0.2$.

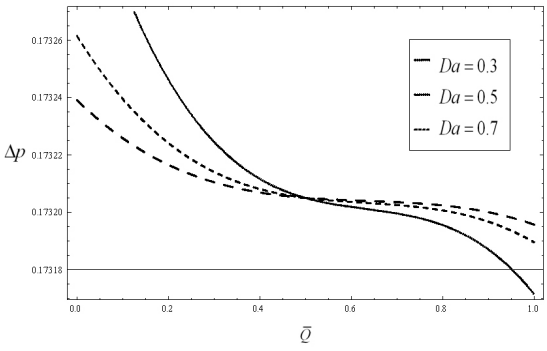

Fig 4. Variation of Δp with $\bar{Q}$ for different values of Da when n =3 , $\alpha = 0.01, \theta = \frac{\pi}{3}, \in = 0.1, \phi = 0.6, \eta = 0.2, \tau = 0.1$

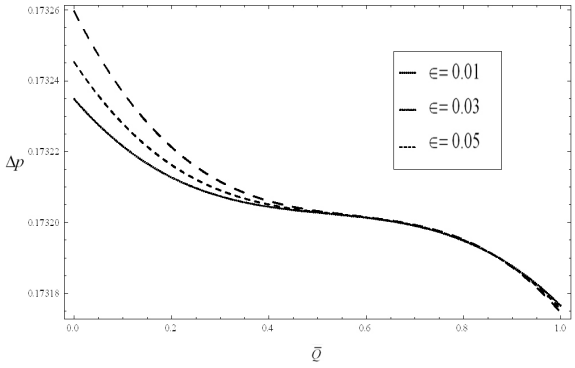

Fig 5. Variation of Δp with $\bar{Q}$ for different values of $\in$ when n=3,Da=0.3, $\alpha = 0.01, \theta = \frac{\pi}{3}, \in = 0.6, \phi = 0.6, \eta = 0.2, \tau = 0.1$

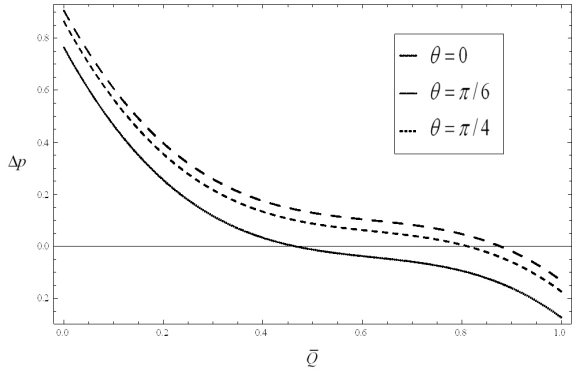

Fig 6. Variation of Δp with $\bar{Q}$ for different values of θ when n = 3, Da = 0.1, $\alpha = 0.1, \in = 0.1, \phi = 0.6, \eta = 0.1, \tau = 0.1$

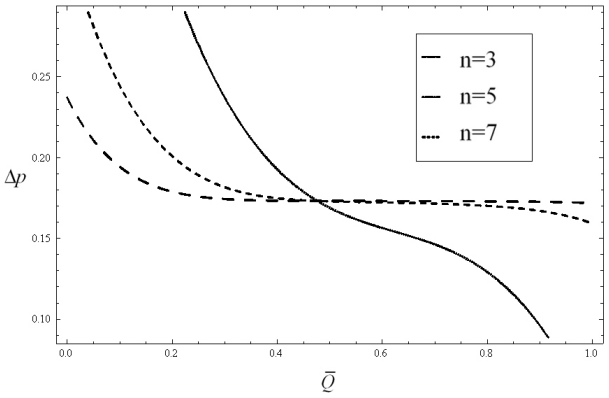

Fig 7. Variation of Δp with $\bar{Q}$ for different values of n when Da= 0.2, $\alpha = 0.1, \in = 0.1, \theta = \pi/3, \phi = 0.6, \eta = 0.1, \tau = 0.2$

ACKNOWLEDGMENT

One of the authors Dr. S. Sreenadh, thanks DST, New Delhi, India for providing financial support through a major research project with No:SR / S4 / MS;503/07.

REFERENCES

[1].T.W.Latham, Fluid motion in peristaltic pumping, M.S.Thesis, MIT, Cambridge, 1966.

[2]. A.H.Shapiro,Pumping and retrograde diffusion in peristaltic waves, Proc. Workshop in ureteral reflux in children, Nat.Acad.Sci., Washington, D.C.,109-126,1967.

[3]. J.C.Burns and T.ParkesPeristaltic motion, J.Fluid Mech., 29, 731-743,1967.

[4]. J.N.Kapur, Mathematical Models in Biology and Medicine, Affiliated East – west press Pvt.Lts,New York,1985.

[5].Y.V.K.RaviKumar, S.V.H.N.KrishnaKumari, M. V. Ramana Murthy, S.Sreenadh. Unsteady peristaltic pumping in a finite length tube with permeable wall, Trans. ASME, Journal of Fluids Engineering,, Vol.32,Pages 1012011 – 1012014,2010.

[6].S.V.H.N.KrishnaKumari.P.,Y.V.K.RaviKumar, M. V. Ramana Murthy, S. Sreenadh, Peristaltic pumping of a Jeffrey fluid under the effect of magnetic field in an inclined channel, Applied Mathematical Sciences, Vol.5 No.9 , Pages 447-458,2011.

[7].S.V.H.N.Krishna Kumari.P.,Y.V.K.Ravi Kumar,M.V.Ramana Murthy,S. Sreenadh, Peristaltic transport of a Jeffrey fluid in the porous tube, ARPN Journal of Engineering and Applied Sciences, Vol.6, No.3, 2011 .

[8]. G.W.Scott Blair , An equation for the flow of blood, Plasma and Serum through glass capillaries, Nature, 183,161,1959.

[9].P.Chaturany.,R.Ponnagalar Sam.,A study of non-Newtonian aspects of blood flow through stenosed arteries and its applications in arterial diseases,Bio.rheol,22,521-531,1985.

[10].K.Vajravelu,S.Sreenadh,V.Ramesh Babu, Peristaltic Transport of Herschel-Bulkley Fluid in an inclined tube, International Journal of Nonlinear Mechanics, vol.40, Issue I,P.83,2005.

[11]. K.Vajravelu,S.Sreenadh,V.Ramesh Babu,Peristaltic pumping of a Herschel-Bulkley fluid in a Channel ,Applied Mathematics and Computation, Vol.169, ,P.726,2005.

Identification Of Acute Appendicitis Using Euclidean Distance On Sonographic Image

R. Balu [1]

Ph.D Research Scholar, Department of Computer Application
School of Computer Science and Engineering,
Bharathiar University, Coimbatore
rvkbalu@yahoo.co.in

T. Devi [2]

Reader and Head i/c, Department of ComputerApplications
School of Computer Science and Engineering,
Bharathiar University, Coimbatore
tdevi5@gmail.com

Abstract: **Acute Abdomen is defined as a syndrome induced by a wide variety of pathological conditions that require emergent medical or more often surgical management. The cardinal presenting symptom is abdominal pain which has many underlying causes. Over the past 10 years, sonography has gained acceptance for examining patients with acute abdominal pain. Sonography is dynamic, noninvasive, rapid, inexpensive, and readily accessible. It is very tedious and time consuming to analyze the sonographic images manually. The authors propose a novel method for diagnosing acute appendicitis using Euclidean distance measures. This paper details the image mining system that automates the diagnosis of acute appendicitis with significant speed up, experimentation methods, real data used for testing and the result.**

Keywords: Image Mining, Euclidean Distance, Data Mining, Appendicitis, Abdomen

I. Introduction

Appendicitis is the most common cause of acute abdominal pain that requires surgical intervention in the Western world [1]. Patients with the disease may present with a wide variety of clinical manifestations, and the diagnosis may elude even the most experienced clinicians [2]. Reginald H. Fitz presented his landmark article in 1886, in which he coined the term ‘‘appendicitis’’ and correctly classified this disease by describing the appendix as the primary source of inflammation in acute typhlitis [3]. Acute Abdomen is defined as a syndrome induced by a wide variety of pathological conditions that require emergent medical or more often surgical management [4].

The cardinal presenting symptom is abdominal pain which has many underlying causes [5-8]. Over the past 10 years, sonography has gained acceptance for examining patients with acute abdominal pain. Sonography is dynamic, noninvasive, rapid, inexpensive, and readily accessible. The impact of sonography on clinical management of patients with an acute abdomen is impressive. Although data can be processed by manual means, it is extremely time consuming and tedious where huge databases and high throughput experiments are involved. Moreover, unlike textual data, images are multidimensional signals, and are communicated to users via 2-D (sometimes 3-D) projections, which may not be straightforward [6]. Image Mining systems can perform these highly valuable tasks after suitable training and testing.

In this work, the authorsdiscuss how Image Mining can aid in diagnosis acute appendicitis in patients who were referred with acute abdominal pain. Retrospective analysis of sonographic imaging features was done.

II. Image mining

Image mining is more than just an extension of data mining to image domain. It is an interdisciplinary endeavor that draws upon expertise in computer vision, image processing, image retrieval, data mining, machine learning, database, and artificial intelligence. Advances in image acquisition and storage technology have led to tremendous growth in very large and detailed image databases [9]. These images, if analyzed, can reveal useful information to the human users. Image mining deals with the extraction of implicit knowledge, image data relationship, or other patterns not explicitly stored in the images. Much knowledge can be obtained from images. This process can be done in the mind by a human, and implementation of this mind processing by a system is very difficult [9].

Image mining has led to tremendous growth in significantly large and detailed image databases. The most important areas belonging to image mining are: image knowledge extraction, content-based image retrieval, video retrieval, video sequence analysis, change detection, model learning, as well as object recognition. Two different types of input data for knowledge extraction from an image collection are original image and symbolic description of the image [10].

III. Appendicitis

Introduction of new imaging technology in particular, graded compression ultrasound andhas changed ‘‘the rules of the game.’’ The adult appendix is a long diverticulum averaging 10 cm in length that arises from the posteromedial wall of the cecum, approximately 3 cm below the ileocecal valve [11]. The appendix may lie in a retrocecal, subcecal, retroileal, preileal, or pelvic site which influences the clinical presentation [12,13].The maximum incidence of the disease occurs in the 2nd decade; thereafter, disease incidence declines with age [14,15]. The primary pathogenic event in the majority of patients with acute appendicitis is luminal obstruction [16-18]. Fecoliths, which result from the inspissations of fecal material and inorganic salts within the appendiceal lumen, are the most common cause of obstruction and are present in 11% – 52% of patients with acute appendicitis [19-21].

Ultrasound is a widely available and inexpensive modality with the potential for highly accurate imaging in the patient suspected to have acute appendicitis. Although operator skill is an important factor in all ultrasound examinations, it has particular importance in the examination of the patient with right-lower-quadrant pain. Nonetheless, the criteria for the US-based diagnosis of acute appendicitis are well established and reliable [22-24]. Ultrasound is also highly useful in identifying an alternate diagnosis [25]. Symptoms of appendicitis usually include pain in the lower right abdomen, loss of appetite, nausea and or vomiting, with or without fever. There may be mild diarrhea or constipation. The site of this pain could be higher in appendicitis in pregnancy, or even lower in those with very long appendix. Early symptoms of appendicitis are those symptoms that most people with this condition may recognize and complain of. They include lower right sided abdominal pain of gradual onset, feeling sick (or nausea), and loss of appetite. Any one with these three symptoms can be assumed to have appendicitis until proven otherwise [26].

IV. Existing Methods for Appendicitis Diagonosis

The diagnosis of appendicitis begins with a thorough history and physical examination. Patients often have an elevated temperature, and there usually will be moderate to severe tenderness in the right lower abdomen when the doctor pushes there. If inflammation has spread to the peritoneum, there is frequently rebound tenderness. Rebound tenderness is pain that is worse when the doctor quickly releases his hand after gently pressing on the abdomen over the area of tenderness[32].

4.1 Leukocytes Count

The white blood cell count in the blood usually becomes elevated with infection. In early appendicitis, before infection sets in, it can be normal, but most often there is at least a mild elevation even early. Unfortunately, appendicitis is not the only condition that causes elevated white blood cell counts. Almost any infection or inflammation can cause this count to be abnormally high. Therefore, an elevated white blood cell count alone cannot be used as a sign of appendicitis[33].

4.2 Urinalysis

Urinalysis is a microscopic examination of the urine that detects red blood cells, white blood cells and bacteria in the urine. Urinalysis usually is abnormal when there is inflammation or stones in the kidneys or bladder. The urinalysis also may be abnormal with appendicitis because the appendix lies near the ureter and bladder. If the inflammation of appendicitis is great enough, it can spread to the ureter and bladder leading to an abnormal urinalysis. Most patients with appendicitis, however, have a normal urinalysis. Therefore, a normal urinalysis suggests appendicitis more than a urinary tract problem.

4.3 Abdominal X-Ray

An abdominal x-ray may detect the fecalith (the hardened and calcified, pea-sized piece of stool that blocks the appendiceal opening) that may be the cause of appendicitis, which is obvious in case of children.

4.4 Ultrasound

An ultrasound is a painless procedure that uses sound waves to identify organs within the body. Ultrasound can identify an enlarged appendix or an abscess. Nevertheless, during appendicitis, the appendix can be seen in only 50% of patients. Therefore, not seeing the appendix during an ultrasound does not exclude appendicitis. Ultrasound also is helpful in women because it can exclude the presence of conditions involving the ovaries, Fallopian tubes and uterus that can mimic appendicitis.

4.5 Barium Enema

A barium enema is an X-ray test where liquid barium is inserted into the colon from the anus to fill the colon. This test can, at times, show an impression on the colon in the area of the appendix where the inflammation from the adjacent inflammation impinges on the colon. Barium enema also can exclude other intestinal problems that mimic appendicitis, for example Crohn's disease.

4.6 Computerized tomography (CT) Scan

In patients who are not pregnant, a CT scan of the area of the appendix is useful in diagnosing appendicitis and peri-appendiceal abscesses as well as in excluding other diseases inside the abdomen and pelvis that can mimic appendicitis [33].

4.7 Laparoscopy

Laparoscopy is a surgical procedure in which a small fiberoptic tube with a camera is inserted into the abdomen through a small puncture made on the abdominal wall. Laparoscopy allows a direct view of the appendix as well as other abdominal and pelvic organs. If appendicitis is found, the inflamed appendix can be removed with the laparoscope. The disadvantage of laparoscopy compared to ultrasound and CT is that it requires a general anesthetic.

There is no one test that will diagnose appendicitis with certainty. Therefore, the approach to suspected appendicitis may include a period of observation, tests as previously discussed, or surgery[33]..

V. Distance Measure

Image processing tools provides various distance transform a metric or measure of the separation of points in the image. Distance Metrics are City Block distance, Chessboard distance and Quasi-Euclidean distance. The city block distance metric measures the path between the pixels based on a 4-connected neighborhood. Pixels whose edges touch are 1 unit apart; pixels diagonally touching are 2 units apart.The chessboard distance metric measures the path between the pixels based on an 8-connected neighborhood. Pixels whose edges or corners touch are 1 unit apart. The quasi-Euclidean metric measures the total Euclidean distance along a set of horizontal, vertical, and diagonal line segments.Image mining tools provides Euclidean distance. The Euclidean distance is the straight-line distance between two pixels. Acute appendicitis is mesure only straight line distance between two pixels.

5. 1 Pre-Processing

The cropping operation and image enhancement can be done to increase the dynamic range of chosen features so that they can be detected easily. The histogram equalization can be used to enhance the contrast within the diognosis of the sonographic images and also hybrid median filtering technique can be used to improve the image quality. Good texture feature extraction can be done by increasing the dynamic range of gray-levels [27].

5.1.1 Texture feature extraction

Though many texture features have been used in the medical image classification, Spatial Gray Level

Dependent Features (SGLDF) can be used to calculate the intersample distance for better diagnosis [28, 29]. In order to detect the abnormalities in medical images association rule mining is built using texture information [30, 31]. This information can be categorized by the spatial arrangement of pixel intensities. In order to capture the spatial distribution of the gray levels within the neighborhood, two dimensional co-occurrence matrices can be applied to calculate the global level features and pixel level features.

5.2 Euclidean distance

In this paper the Appendicitis is found out using the Distance measure in order to confirm the patient is diagnosis with Appendices. The distance is the predominant one to bring out the diagnosis. The Euclidean distance is used here to find out the measure of the acute appendicitis.

Euclidean distance is the distance between two points in Euclidean space. Take two points P and Q in two dimensional Euclidean spaces. This describes P with the coordinates (p1,p2) and Q with the coordinates (q1,q2). Now construct a line segment with the endpoints of P and Q. This line segment will form the hypotenuse of a right angled triangle. The distance between two points p and q is defined as the square root of the sum of the squares of the differences between the corresponding coordinates of the points; for example, in two-dimensional Euclidean geometry, the Euclidean distance between two points a = (ax, ay) and b = (bx, by) is defined as:

$$d(a,b) = \sqrt{(p_1 - q_1)^2 + (p_2 - p_2)^2}$$

This algorithm computes the minimum Euclidean distance between a column vector x and a collection of column vectors in the codebook matrix cb. The algorithm computes the minimum distance to x and finds the column vector in cb that is closest to x. It outputs this column vector, y, its index, idx, in cb, and distance, the distance between x and y.

Step1: load the column vector x;
Step2: load the code book;
Step3: minimum distance is initially set to the first element of cb.
Step4: i.e. set idx=1;
Step5: compute distance by normalized values of (x-cb) for all cb;
Step6: if d is lessthan distance set distance is equal to d;
Step7: set idx=index;
Step8; end

Fig 1: Proposed method

$$d(a,b) = |p - q|$$

$$\sqrt{(p_1 - q_1)^2 + (p_2 - q_2)^2 + \cdots + (p_n - q_n)^2}$$

$$= \sqrt{\sum_{i=1}^{n} (p_i - q_i)^2}$$

In one dimension, the distance between two points, x1 and x2, on a line is simply the absolute value of the difference between the two points: [32]

$$\sqrt{(X_2 - X_1)^2} = |X_2 - X_1|$$

In two dimensions, the distance between

P = (p_1,p_2) and q = (q_1,q_2) is:

$$\sqrt{(p_1 - q_1)^2 + (p_2 - p_2)^2}$$

The example for this tutorial computes the minimum Euclidean distance between a column vector x and a collection of column vectors in the codebook matrix cb. The function has three output variables:

- y, the vector in cb with the minimum distance to x
- idx, the index of the column vector in cb corresponding to the closest vector
- distance, the distance between x and y

Fig 2: Sonographic image of Appendicitis

Fig 3: Distance Measure

Table1: Variables for Distance Measure.

Name	Size	Bytes	Class
Distance	1x1	8	double
Point1	1x2	16	double
Point2	1x2	16	double

VI. Experimental Study

An experiment has been conducted on sonography data set based on the proposed algorithm is shown in fig1.The original input image is shown in Fig2. The result for finding acute appendicitis by distance measure is shown in fig3.The proposed algorithm has been used to determine the acute appendicitis using the distance measure as shown in fig3.

The study period was from Jan 2010 – May 2010. Ultrasound imaging was done in all patients. Patients were followed up until the discharge diagnosis was made. Acute appendicitis of sonographic imaging findings in 148 patients was done in patients. In the experimental study total number of 148 instances has been studied in the range of 16 – 51 years. It is noted that mean age of these referel instances are the range 33 – 34. Male and female sex ratio is in the range of 2 : 1. The column chart clearly shows the sex distribution for 148 instances.

6.1 Results

The images are classified in two different sizes based on the thickness of appendicitis with *greater than 6 mm* and *less than 6 mm*. The proposed system is tested with 148 instances and the results obtained are: out of 148 instances, 124 instances show thickness measured as greater than 6 mm. Table 2 shows the results out of the the experimental study conducted for finding acute appendicitis using sonographic images from 148 patients.

Table 2 : Thickness of Appendix

Size	No. of Patients	Percentage
≥ 6 mm	124	83.78%
< 6 mm	24	16.22%

Graph 1 : Thickness of Appendix

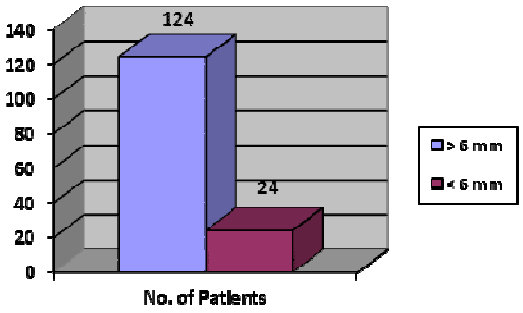

A sonologist has been consultated and the results obtained from the sonologist on the same 148 samples reveal that 119 patients are affected by appendicitis. A comparison of the results obtained from the proposed system with the results obtained from the sonologist has been done and the results are as shown in table 3 and the graph corresponding to this is shown in graph 2.

Table3: Comparison of Proposed Method and Real Result

Size	Results from Proposed method	Results from Sonologist
≥ 6 mm	124	119
< 6 mm	24	29

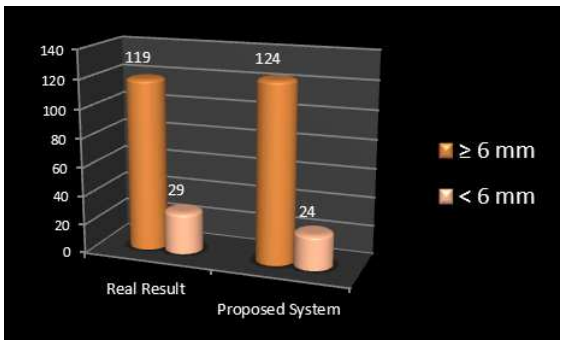

Graph 2 : Comparison of Real Result and Proposed Method

6.2 Validation of Results

The results are validated by calculating the deviation of the results obtained through the proposed method and the real results obtained from the sonologist. The calculations are shown in table 4.

Table4: Difference between the results

N = 148	Results from Proposed method	Results from Sonologist	Difference
Mean	0.84	0.80	0.03
Varience	103.89	95.68	8.21
Std Dev	10.19	9.78	0.41
Std Err	0.26	0.26	0.00

The standard deviation and standard error clearly show that the proposed method yields nearly good results.

VII. Conclusion

In this paper, a new algorithm has been proposed to measure the distance for finding the aucte appendicitis. The quasi-euclidean metric measures the total euclidean distance along a set of horizontal, vertical and diagonal line segments. The existence of appendicitis is found out using the distance measure on the sonographic image of the patient who is diagnosed for appendicitis. Out of the 148 patients considered for experimental study, 124 sonographic images showed a length of above 6 mm implying the existence of appendicitis. The euclidean distance is used here to find out the measure of the acute appendicitis. This work can be further extended to include the module on automatic identification of the start and end points of measurement using image processing and automation techniques.

VIII. References

1 R. Brooke Jeffrey, Jr., MD, Faye C. Laing, MD Frank R. Lewis, MD. Acute Appendicitis: High-Resolution Real-Time US Findings, Radiology 1987; 163:11-14.

2 Williams GR. Presidential address: history of appendicitis, with anecdotes illustrating its importance. Ann Surg 1983; 197:495–506.

3 Fitz RH. Perforating inflammation of the vernzmiform appendix, with special reference to its early diagnosis and treatment.Trans Assoc Am Physicians 1886; 1:107–144.

4 H. Prasad, G. Rodrigues & R. Shenoy : Role Of Ultrasonography In Non Traumatic Acute Abdomen . The Internet Journal of Radiology. 2007 Volume 5 Number 2

5 Sturman MF. Medical imaging in acute abdominal pain. Compr Ther 1991; 17:15-21.

6 Brewer BJ, Golden GT, Hitch DC, Rudolph LE, Wangensteen SL. Abdominal pain: an analysis of 1,000 consecutive cases in a university hospital setting. Am J Surg 1976; 131:219-223.

7 DeDombal FT. Diagnosis of acute abdominal pain 2nd ed. New York, NY: Churchill Livingstone, 1991.

8 Anyanwu AC, Moalypour SM. Are abdominal radiographs still overutilized in the assessment of acute abdominal pain? A district general hospital audit. J R Coll Surg Edinb 1998; 43:267-270.

9 Wynne Hsu, Mong Li Lee,Ji Zhang , " Image Mining: Trends and Developments Journal of Intelligent Information Systems archive, Volume 19 , Issue 1 Pages: 7 - 23 ,2002 .

10 Rokia Missaoui, Roman M. Palenichka, "Effective image and video mining: an overview of model-based approaches", Pages: 43 - 52 , 2005.

11 Buschard K, Kjaeldfaard A. Investigation and analysis of the position, fixation, length and embryology of the vermiform appendix. Acta Chir Scand 1973; 139:293–298.

12 Guidry SP, Poole GV. The anatomy of appendicitis. Am Surg 1994; 60:68–71.

13 Wagner JM, McKinney P, Carpenter JL. Does this patient have appendicitis? JAMA 1996; 276:1589–1594.

14 Addiss DG, Shaffer N, Fowler BS, Tauxe RV. The epidemiology of appendicitis and appendectomy in the United States. Am J Epidemiol 1990; 132:910–925.

15 Primatesta P, Goldacre MJ. Appendicectomy for acute appendicitis and for other conditions: an epidemiological study. Int J Epidemiol 1994; 23:155–160.

16 Bowers WF. Appendicitis: with special reference to pathogenesis, bacteriology and healing. Arch Surg 1939; 39:362–422.

17 Wangensteen OH, Dennis C. Experimental proof of the obstructive origin of appendicitis in man. Ann Surg 1939; 110:629–647.

18 Pieper R, Kager L, Tidefeldt U. Obstruction of the appendix vermiformis causing acute appendicitis: an experimental study in the rabbit. Acta Chir Scand 1982; 148:63–72.

19 Nitecki S, Karmeli R, Sarr MG. Appendiceal calculi and fecaliths as indications for appendectomy. Surg Gyn Obstet 1990; 171:185–188.

20 Jones BA, Demetriades D, Segal I, Burkitt DP. The prevalence of appendiceal fecaliths in patients with and without appendicitis: a comparative study from Canada and South Africa. Ann Surg 1985; 202: 80–82.

21 Shaw RE. Appendix calculi and acute appendicitis. Br J Surg 1965; 52:451–459.

22 Jeffrey RB Jr, Laing FC, Townsend RR. Acute appendicitis: sonographic criteria based on 250 cases. Radiology 1988; 167:327–329.

23 Birnbaum BA, Jeffrey RB Jr. CT and sonographic evaluation of acute right lower quadrant pain. AJR Am J Roentgenol 1998; 170:361–371.

24 Puylaert JB. Acute appendicitis: US evaluation using graded compression. Radiology1986; 158:355–360.

25 Gaensler EHL, Jeffrey RB Jr, Laing FC, Townsend RR. Sonography in patients with suspected acute appendicitis: value in establishing alternative diagnoses. AJR Am J Roentgenol 1989; 152:49–51

26 Signs and Symptoms of Appendicitis at http://www.abdopain.com/symptoms-of-appendicitis.html

27 J.C. Felipe, A.J.M Traina, and C. Traina, "Retrieval by content of medical images using texture for tissue identification," In Proc: 16th IEEE Symp. Computer-Based Med. Systems. CBMS 2003, pp. 175–180.

28 L. Hui, W. Hanhu, C. Mei, and W. Ten , "Clustering Ensemble Technique Applied in the Discovery and Diagnosis of Brain Lesions," In Proc: Sixth International Conference on Intelligent Systems Design and Applications (ISDA) , vol. 2: 2006, pp. 512-520.

29 C.F. Joaquim, X.R. Marcela, P.M.S. Elaine, J.M.T. Agma, and T.J. Caetano, "Effective shape-based retrieval and classification of mammograms," In Proc: ACM symposium on Applied computing, 2006, pp. 250 – 255.

30 N.R. Mudigonda, R.M. Rangayyan , "Detection of breast masses in mammograms by density slicing and texture flow-field analysis," IEEE Trans. Med. Imag. 20(12), 2001, pp. 1215–1227.

31 K. Murat, I.M. Cevdet,"An expert system for detection of breast cancer based on association rules and neural network," An International Journal Expert Systems with Applications 36: 2009, pp. 3465–3469.

32 http://en.wikipedia.org/wiki/Euclidean_distance

33 E.Sivasankar, Dr.R.S.Rajesh and Dr.S.Venkateswaran, "Diagnosing Appendicitis Using Backpropagation Neural Network and Bayesian Based Classifier", International Journal of Computer Theory and Engineering, Vol. 1, No. 4, October, 2009 1793-8201

34 Appendicitis at http://www.medicinenet.com/ appendicitis/page2.htm

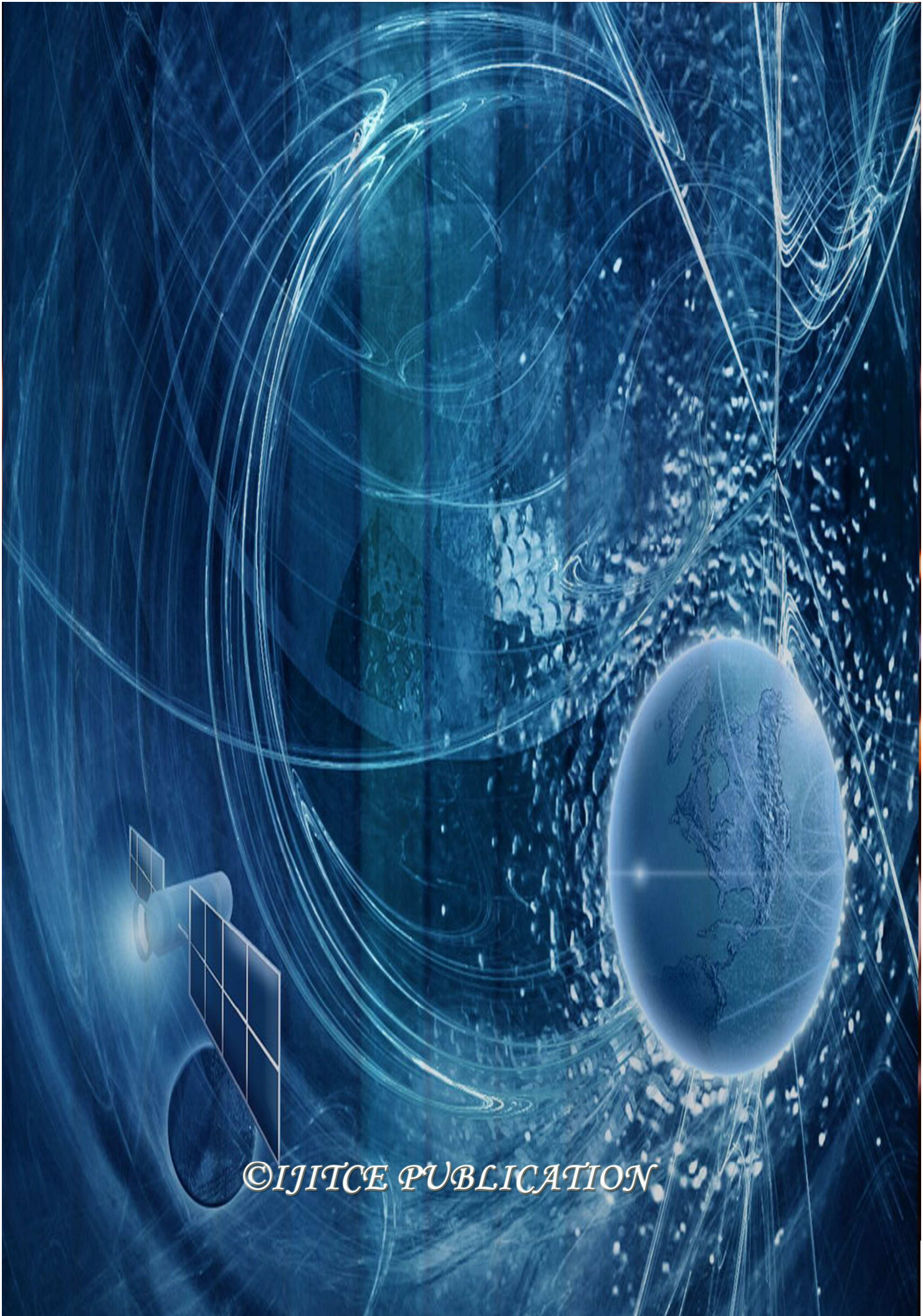
©IJITCE PUBLICATION